

REVIEW ARTICLE

On correlation effects in electron spectroscopies and the *GW* approximation

To cite this article: Lars Hedin 1999 *J. Phys.: Condens. Matter* **11** R489


View the [article online](#) for updates and enhancements.

Related content

- [The *GW* method](#)
F Aryasetiawan and O Gunnarsson
- [A New Approach to the Theory of Photoemission from Solids](#)
W Bardyszewski and L Hedin
- [Dynamical screening in correlated electron systems—from lattice models to realistic materials](#)
Philipp Werner and Michele Casula

Recent citations

- [Cumulant Green's function calculations of plasmon satellites in bulk sodium: Influence of screening and the crystal environment](#)
Jianqiang Sky Zhou *et al*
- [A Comparison between Bethe-Salpeter Equation and Configuration Interaction Approaches for Solving a Quantum Chemistry Problem: Calculating the Excitation Energy for Finite 1D Hubbard Chains](#)
Qi Ou and Joseph E. Subotnik
- [Finite Temperature Green's Function Approach for Excited State and Thermodynamic Properties of Cool to Warm Dense Matter](#)
J. J. Kas and J. J. Rehr



Instruments for Advanced Science


Contact Hiden Analytical for further details:
W www.HidenAnalytical.com
E info@hiden.co.uk

CLICK TO VIEW our product catalogue




Gas Analysis

- dynamic measurement of reaction gas streams
- catalysis and thermal analysis
- molecular beam studies
- dissolved species probes
- fermentation, environmental and ecological studies




Surface Science

- UHV-TPD
- SIMS
- end point detection in ion beam etch
- elemental imaging - surface mapping



Plasma Diagnostics

- plasma source characterization
- etch and deposition process reaction kinetic studies
- analysis of neutral and radical species



Vacuum Analysis

- partial pressure measurement and control of process gases
- reactive sputter process control
- vacuum diagnostics
- vacuum coating process monitoring

REVIEW ARTICLE

On correlation effects in electron spectroscopies and the *GW* approximation

Lars Hedin

Department of Theoretical Physics, Lund University, Sölvegatan 14A, 223 62 Lund, Sweden
and
Max-Planck Institut für Festkörperforschung, Heisenbergstrasse 1, D-70569 Stuttgart, Germany

Received 28 June 1999

Abstract. The *GW* approximation (GWA) extends the well-known Hartree–Fock approximation (HFA) for the self-energy (exchange potential), by replacing the bare Coulomb potential v by the *dynamically screened potential* W , e.g. $V_{ex} = iGv$ is replaced by $\Sigma_{GW} = iGW$. Here G is the one-electron Green's function. The GWA like the HFA is self-consistent, which allows for solutions beyond perturbation theory, like say spin-density waves. In a first approximation, iGW is a sum of a statically screened exchange potential plus a Coulomb hole (equal to the electrostatic energy associated with the charge pushed away around a given electron). The Coulomb hole part is larger in magnitude, but the two parts give comparable contributions to the dispersion of the quasi-particle energy. The GWA can be said to describe an *electronic polaron* (an electron surrounded by an electronic polarization cloud), which has great similarities to the ordinary polaron (an electron surrounded by a cloud of phonons). The dynamical screening adds new crucial features beyond the HFA. With the GWA not only bandstructures but also spectral functions can be calculated, as well as charge densities, momentum distributions, and total energies. We will discuss the ideas behind the GWA, and generalizations which are necessary to improve on the rather poor GWA satellite structures in the spectral functions. We will further extend the GWA approach to fully describe spectroscopies like photoemission, x-ray absorption, and electron scattering. Finally we will comment on the relation between the GWA and theories for strongly correlated electronic systems. In collecting the material for this review, a number of new results and perspectives became apparent, which have not been published elsewhere.

Contents

1. Introduction
2. The one-electron Green's function G and its spectral function A
 - 2.1. Some general definitions and exact relations
 - 2.2. The self-energy Σ and the quasi-particle energies
 - 2.3. The spectral function and photoemission
3. The *GW* approximation to the self-energy
 - 3.1. General expressions
 - 3.2. The Coulomb hole plus screened exchange approximation; limiting cases
 - 3.3. Comments on the RPA, r_s -expansions, and vertex corrections
4. Electron–boson model Hamiltonians and fluctuation potentials
 - 4.1. Introduction
 - 4.2. The core-electron spectrum
 - 4.3. Valence-electron spectra

5. Photoemission theory beyond the sudden approximation
 - 5.1. General aspects
 - 5.2. Photoemission in the high-energy limit and fluctuation potentials
 - 5.3. Core-electron photoemission in metals
 - 5.4. Strongly correlated systems
6. Concluding remarks

1. Introduction

The GW approximation (GWA) to the one-electron self-energy, $\Sigma = iGW$ [1, 2], has been very successful in accounting for *quasi-particle* (QP) energies for a wide range of solids, as well as for isolated atoms. An early compact review of the GWA was written by Hybertsen and Louie [3], and recently there have been more detailed reviews [4–6]. There is no reason to add another detailed discussion of the technical aspects, and the results obtained with the GWA. Instead this short review focuses on the main physical ideas, and on extensions of these ideas to spectroscopies [7–14].

At first sight the electron correlation problem for solids looks completely intractable. The electrons are on average some Bohr radii (a_0) apart, and thus have an interaction energy of $e^2/a_0 = 1$ au (27.2 eV). This is some two orders of magnitude larger than the energy accuracy we need for a meaningful discussion of say bandstructures or impurity levels. The electron interactions are too large to allow a low-order perturbation treatment, and the number of electrons is too large to allow a full calculation including all inter-electron interactions. For some reasons which we will discuss later, one-electron mean-field descriptions can however go a long way in accounting for important features of these strong interactions.

There is no straightforward well-controlled way to obtain good quantitative results for correlations. We must think hard on what the essential ingredients in a specific type of problem are, and make appropriate approximations. We then seldom have a chance to make error estimates in a mathematical sense. Instead, progress builds on using reasonable approximations and obtaining systematic agreement with experiment. As an example, think of the BCS theory of superconductivity. Here the effects are on the meV ($\approx 1/30\,000$ au) scale or smaller, while the absolute errors in the energies are many orders of magnitude larger. Still the BCS theory has caught the essential features, and gives a marvellous description of (normal) superconductivity.

For a large class of problems, the necessary starting point for treating correlation is finding a good set of one-electron orbitals, calculated with some sort of effective field that includes Coulomb forces self-consistently. Already the Hartree approximation correctly gives to a large extent the important trends. The Hartree approximation however includes the large orbital self-interactions, which are cancelled by the exchange terms in the Hartree–Fock approximation (HFA). However, the HFA only includes correlation between electrons through the Pauli principle, and there are no effects of correlation between electrons of opposite spin. Today, calculations based on density functional theory (DFT) using the local density approximation (LDA) dominate. In principle these calculations include correlation effects, but the exchange–correlation potential is often not good enough to fully cancel the orbital self-interactions. This has led to schemes like that of the SIC (self-interaction-corrected) local density potentials. DFT is primarily a theory that applies to ground-state properties, but it can be extended to treat excited states [15].

The self-energy operator Σ allows us to obtain QP states, and thus bandstructure energies. Here we will in particular concentrate on the GW approximation for the self-energy. It resembles the HF exchange term, which is also a non-local operator. Fortunately the orbitals

obtained with the HFA, the LDA, and the GWA are often very close [16]. Thus in many cases one can obtain good GW results by solving a LDA problem, and then take the expectation value of the GW self-energy. This gives a substantial simplification both as regards numerical evaluations and as regards the discussion of the results. The main reason behind this closeness of the orbitals is of course that the Coulomb potential is a dominating part, and a potential that accounts reasonably well for the orbital self-interaction effects gives good orbitals. The Σ operator, unlike the HF exchange operator, has an energy dependence which leads to a description of correlation effects in spectroscopies like photoemission beyond the Landau QP picture.

When we discuss solids, we find that s and p orbitals are distinctly different from d and f orbitals; s and p orbitals on different atoms (at normal pressures) overlap substantially, while the overlap between d and f orbitals is much smaller. In the first case the occupation numbers of plane-wave-like states are a natural ingredient, while in the second a tight-binding picture and occupation numbers of localized states are more relevant (cf. p 281 of [17]).

Hence one can talk of sp solids, and of df solids. The localization of the d and f orbitals makes the correlation problem fundamentally different. For sp solids the correlation is set by long-range charge-density (e.g. plasmon) oscillations. For df solids, the energy cost for double occupancy is high, and it is even meaningful to exclude double occupancy—that is, to completely freeze out the charge fluctuations. This can be done in say a Hubbard model by letting the Hubbard U approach infinity. In a half-filled one-band Hubbard model, the electrons then cannot move at all, and the only remaining degree of freedom is the orientation of the spin (a *Mott–Hubbard insulator*). A classical treatment would give a definite spin-ordered pattern. Also a quantum treatment leads to strong spin correlations, which persist at small doping.

Clearly the GWA describing long-range charge fluctuations, and a Hubbard model focusing on local on-site correlations, which drive strong spin correlations, are two extremes. The GWA has the advantage that it describes the charge fluctuations including details of the band-structure, which are hard to include in a Hubbard model. Since effects of charge movement are very strong, it is important to have a detailed description of them. In the Hubbard model the on-site repulsion energy U is hard to estimate. Often one estimates U by making constrained-configuration LDA ground-state calculations. U is found to deviate by a factor of two or more from its free-atom value, a deviation caused by charge rearrangements or screening in the solid. An additional problem with the Hubbard model is that U is taken as a constant, while intuitively we expect the effective U to vary with the state that we are describing, particularly if different states involve different charge distributions. An important drawback for Hubbard–Anderson types of model is that they are parametrized, and there is no secure way to establish the parameters. And even if we judge that our estimates of the parameters are good, we are still limited by the very restricted form of the models.

In sp solids, correlation effects are not immediately striking, while for the df solids, they are glaringly present. This does not mean that they are small for sp solids; it just means that simple models can work well. Thus we can easily have correlation shifts of some 10 electron volts, but still obtain the topology of the bands and Fermi surfaces fairly well without correlation. Still, sp systems are often called weakly, and df systems strongly correlated.

Let us recall Fermi-liquid theory. When it is valid, it concerns low-energy excitations and low temperatures. The fundamental excitations are QPs. They have a finite lifetime, which for small energies is very long. When Fermi-liquid theory applies, we talk of normal systems. A small bandwidth does not necessarily mean non-Fermi-liquid behaviour. Rare-earth compounds can have very narrow bands, and still be good metals and Fermi liquids at low temperatures, when a coherent motion is possible. Particularly low-dimensional systems may however not be Fermi liquids—such as Luttinger-liquid systems in 1D (and perhaps 2D),

and the 2D electron gas in high magnetic fields (Laughlin states).

Often one talks loosely of one-electron and of correlated behaviour. Then band theory is considered an uncorrelated one-electron theory, and correlation is taken as synonymous with descriptions by model Hamiltonians, like those of Hubbard and Anderson. From our previous discussions we see that this is oversimplified and misleading terminology.

One useful concept for discussing correlation effects is the one-electron Green's function, G . This function defines a self-energy Σ , and vice versa; schematically,

$$[E - h - \Sigma(E)]G(E) = 1$$

where h is the one-electron operator which includes the kinetic energy, and the Coulomb potential from the nuclei and from the average of the electron charge density (the Hartree potential). G is always well defined, even for exotic states and high temperatures. G also has a close connection to QPs, if we have a normal solid. The QPs are obtained from the homogeneous equation

$$[E - h - \Sigma(E)]\psi = 0.$$

This equation does indeed have a one-electron form, but the operator Σ has very non-trivial correlation effects built in, and is far from a mean-field approximation. G is also closely related to fundamental properties, like photoemission, charge and spin densities, and total energies. Thus e.g. photoemission is, to a first approximation, given by the spectral function

$$A(\omega) = (1/\pi) \text{Im} G(\omega) = (1/\pi) \text{Im}[\omega - h - \Sigma(\omega)]^{-1}$$

and thus related to the energy dependence of Σ .

The main ingredients in the GWA are the Green's function G , which depends on the one-electron energies and wavefunctions, and the dynamically screened potential W , which depends on boson-type excitation energies and charge-fluctuation potentials (e.g. from particle-hole pairs and plasmons). The dynamical screening is here discussed within the RPA. This approximation has turned out to be generally very good, as illustrated by the results for the electron-phonon problem [18].

The GWA results can be obtained in first-order perturbation theory from a model Hamiltonian with electrons coupled to bosons, where all parameters are extracted from the ingredients in G and W . This fact lends itself to generalizations with similar model Hamiltonians which can describe physics outside the range of the one-electron Green's function, like spectroscopies such as photoemission, x-ray absorption, and electron scattering. Discussions of such generalizations form an important part of this article.

2. The one-electron Green's function G and its spectral function A

2.1. Some general definitions and exact relations

The one-electron Green's function is a central quantity in many approaches to describing electronic structure [19]. It is defined (at zero temperature) as an expectation value with respect to the ground-state many-electron function, $|N\rangle$:

$$\begin{aligned} G(xt, x't') &= -i\langle N|T\psi(xt)\psi^\dagger(x't')|N\rangle \\ &= \begin{cases} -i\langle N|\psi(x)e^{-i(H-E(N))(t-t')}\psi^\dagger(x')|N\rangle & t > t' \\ i\langle N|\psi^\dagger(x')e^{i(H-E(N))(t-t')}\psi(x)|N\rangle & t < t'. \end{cases} \end{aligned}$$

Here $\psi(xt)$ is the field operator, x stands for three space coordinates (\mathbf{r}) and one spin coordinate (ξ), and T is the time-ordering operator. The Fourier transform with respect to time is (we use

atomic units, $e = \hbar = m = 1$, and thus e.g. the energy is in Hartree units, 27.2 eV)

$$G(x, x'; \omega) = \int_{-\infty}^{\infty} e^{i\omega t} G(xt, x't) dt = \int_C \frac{A(x, x'; \omega')}{\omega - \omega'} d\omega' \quad (1)$$

where

$$A(x, x'; \omega) = \sum_s f_s(x) f_s^*(x') \delta(\omega - \varepsilon_s) \quad (2)$$

$$f_s(x) = \begin{cases} \langle N | \psi(x) | N+1, s \rangle & \text{for } \varepsilon_s \equiv E(N+1, s) - E(N) > \mu \\ \langle N-1, s | \psi(x) | N \rangle & \text{for } \varepsilon_s \equiv E(N) - E(N-1, s) < \mu. \end{cases} \quad (3)$$

The contour C runs just above the real axis for $\omega' < \mu$, and just below for $\omega' > \mu$, where μ is the chemical potential. Introducing a complete set of orthonormal one-electron wavefunctions $\{\phi_i\}$, we have

$$A_{ij}(\omega) = \sum_s \langle i | s \rangle \langle s | j \rangle \delta(\omega - \varepsilon_s). \quad (4)$$

From the definition of G it follows that

$$\int_{-\infty}^{\infty} A(x, x'; \omega) d\omega = \delta(x - x') \quad (5)$$

$$\rho(\mathbf{r}) = -i \int G(xt, xt^+) d\xi = \text{charge density}$$

$$E = \frac{1}{2} \sum_{ij} \int_{-\infty}^{\mu} [\omega \delta_{ij} + h_{ij}] A_{ji}(\omega) d\omega + V_{nn} = \text{total energy.}$$

Here V_{nn} is the energy of interaction between the bare nuclei, and

$$A_{ij}(\omega) = \int \phi_i^*(x) A(x, x') \phi_j(x') dx dx' \quad (6)$$

$$h_{ij} = \int \phi_i^*(x) h \phi_j(x) dx \quad h = -\frac{\nabla^2}{2} + V_{nucl} + V_H$$

$$V_{nucl} = -\sum_n \frac{Z_n}{|\mathbf{r} - \mathbf{R}_n|} \quad V_H = \int \frac{\rho(\mathbf{r}') d\mathbf{r}'}{|\mathbf{r} - \mathbf{r}'|}. \quad (7)$$

V_H is the Hartree potential. A also gives the distribution of one-electron states:

$$n_i = \langle N | c_i^\dagger c_i | N \rangle = \int_{-\infty}^{\mu} A_{ii}(\omega) d\omega.$$

With the state i being a momentum state, we obtain the momentum distribution, a key quantity in e.g. Compton scattering. We have defined the Green's function for the zero-temperature case. It is straightforward to generalize the results to finite temperatures.

2.2. The self-energy Σ and the quasi-particle energies

We define the self-energy Σ by

$$G^{-1}(x, x'; \omega) = [\delta(x - x')(\omega - h(x')) - \Sigma(x, x'; \omega)].$$

From equations (1) and (2), and noting that $G^{-1}G = 1$, we have

$$\int [\delta(x - x'')(\omega - h(x'')) - \Sigma(x, x''; \omega)] \sum_s \frac{f_s(x'') f_s^*(x')}{\omega - \varepsilon_s} dx'' = \delta(x - x').$$

When s is a discrete level, we can take the $\omega \rightarrow \varepsilon_s$ limit to find [1]

$$\int [\delta(x - x'')(\varepsilon_s - h(x'')) - \Sigma(x, x''; \varepsilon_s)] f_s(x'') dx'' = 0.$$

In a schematic notation we have to solve the eigenvalue problem

$$[\varepsilon - h - \Sigma(\varepsilon)]f = 0. \tag{8}$$

This is often called the Dyson equation for the QP energies ε and amplitudes f . The Dyson equation is a single-particle equation, and reduces to the Hartree–Fock (HF) equation if we replace the self-energy $\Sigma(x, x'; \omega)$ by the HF exchange potential $V_{ex}(x, x')$. Both are non-local but Σ is in addition energy dependent. For energy ranges where the ε_s form a continuum, $\Sigma(x, x'; \omega)$ is also complex. Equation (8) then still has a solution with a complex ε , when we use an analytical continuation of $\Sigma(\omega)$. **The real parts of the solutions to the Dyson equation give us the bandstructures, and the imaginary parts the QP damping.**

When we neglect the non-diagonal parts in G and Σ we have

$$G_i(\omega) = \frac{1}{\omega - \varepsilon_i - \Sigma_i(\omega)} \tag{9}$$

where $\varepsilon_i = h_{ii}$ and $\Sigma_i = \Sigma_{ii}$. From equation (1) we then have

$$G_i(\omega) = \int_C \frac{A_i(\omega')}{\omega - \omega'} d\omega'$$

and

$$A_i(\omega) = \frac{1}{\pi} |\text{Im } G_i(\omega)| = \frac{1}{\pi} \frac{|\text{Im } \Sigma_i(\omega)|}{(\omega - \varepsilon_i - \text{Re } \Sigma_i(\omega))^2 + (\text{Im } \Sigma_i(\omega))^2}.$$

We expand equation (9) for ω close to the QP energy E_i :

$$G_i(\omega) = \frac{1}{\omega - \varepsilon_i - [\Sigma_i(E_i) + (\omega - E_i)(\partial \Sigma_i(\omega)/\partial \omega)|_{\omega=E_i} + \dots]} \approx \frac{Z_i}{\omega - E_i}$$

with

$$E_i = \varepsilon_i + \Sigma_i(E_i) \quad Z_i = \frac{1}{1 - (\partial \Sigma_i(\omega)/\partial \omega)|_{\omega=E_i}}.$$

The spectral function for ω close to E_i is then

$$A_i(\omega) = \frac{1}{\pi} \frac{|\text{Im } E_i \text{ Re } Z_i + (\omega - \text{Re } E_i) \text{Im } Z_i|}{(\omega - \text{Re } E_i)^2 + (\text{Im } E_i)^2}.$$

If $|\text{Im } E_i|$ is small, $A_i(\omega)$ has a sharp Fano peak at $\omega = \text{Re } E_i$ of width $\Gamma_i = |\text{Im } E_i|$ and strength $|\text{Re } Z_i|$, with the asymmetry set by $\text{Im } Z_i$. From equation (5) it follows (also when the non-diagonal elements do not vanish) that

$$\int_{-\infty}^{\infty} A_i(\omega) d\omega = 1.$$

Even for weakly correlated systems like sp metals and valence semiconductors, $|\text{Re } Z_i|$ is far from 1, and can be say 0.6–0.8. The region outside the QP peak is called the *incoherent* or *satellite* structure. For sp systems it can be dominated by a fairly sharp plasmon peak.

2.3. The spectral function and photoemission

There is a close relation between the spectral function A and the sudden approximation for photoemission. The exact expression for the photocurrent J_k can be written in golden rule form [20]:

$$J_k(\omega) = \sum_s |\langle N-1, s; \mathbf{k} | \Delta | N \rangle|^2 \delta(\varepsilon_k - \varepsilon_s - \omega). \quad (10)$$

Here $\langle N-1, s; \mathbf{k} |$ is the final state with a photoelectron in a time-inverted scattering state having a momentum \mathbf{k} , and the solid in an excited state s , and

$$\Delta = \sum_{ij} \Delta_{ij} c_i^\dagger c_j$$

is the dipole transition operator. In the sudden approximation we take the photoelectron as decoupled from the target:

$$|N-1, s; \mathbf{k}\rangle = c_k^\dagger |N-1, s\rangle. \quad (11)$$

If we further neglect virtual fluctuations in the ground state $|N\rangle$ which involve the one-particle state $|\mathbf{k}\rangle$, we can put $c_k c_i^\dagger = \delta_{ki}$ and we have [19]

$$\langle N-1, s | c_k \sum_{ij} \Delta_{ij} c_i^\dagger c_j | N \rangle = \sum_j \Delta_{kj} \langle N-1, s | c_j | N \rangle.$$

From equation (4), when $\omega < \mu$ we have

$$A_{ij}(\omega) = \sum_s \langle N-1, s | c_i | N \rangle \langle N | c_j^\dagger | N-1, s \rangle \delta(\omega - \varepsilon_s)$$

which leads to

$$J_k(\omega) = \sum_{ij} \Delta_{ki} A_{ij}(\varepsilon_k - \omega) \Delta_{jk}. \quad (12)$$

Keeping only the diagonal elements in A_{ij} , we have

$$J_k(\omega) = \sum_i |\Delta_{ki}|^2 A_{ii}(\varepsilon_k - \omega).$$

It is common also to take the dipole matrix element as constant, when estimating the photoemission current. For independent particles, $A_{ij}(\omega) = \delta_{ij} \delta(\omega - \varepsilon_i)$, which gives the well-known one-electron expression

$$J_k(\omega) = \sum_i^{occ} |\Delta_{ki}|^2 \delta(\varepsilon_k - \varepsilon_i - \omega).$$

3. The GW approximation to the self-energy

3.1. General expressions

As a starting point we recall the expression for the Hartree–Fock Hamiltonian. Schematically we have

$$h_{HF} = h + V_{ex}$$

where V_{ex} is the exchange potential:

$$V_{ex}(x, x'; \omega) = \frac{1}{|\mathbf{r} - \mathbf{r}'|} \frac{i}{2\pi} \int e^{i\delta\omega'} G_0(x, x'; \omega') d\omega' = -\frac{1}{|\mathbf{r} - \mathbf{r}'|} \sum_i^{occ} \phi_i(x) \phi_i^*(x').$$

The zero-order Green's function is

$$G_0(x, x'; \omega) = \sum_i \frac{\phi_i(x)\phi_i^*(x')}{\omega - \varepsilon_i + i\delta \operatorname{sgn}(\varepsilon_i - \mu)}$$

As a comparison, the Kohn–Sham and *GW* Hamiltonians can be written as

$$h_{KS} = h + V_{xc} \quad h_{GW} = h + \Sigma_{GW}$$

Explicitly we have

$$\Sigma_{GW}(x, x'; \omega) = \frac{i}{2\pi} \int e^{i\delta\omega'} G(x, x'; \omega') W(\mathbf{r}, \mathbf{r}'; \omega - \omega') d\omega'. \quad (13)$$

For this reason, one may also call the GWA a *dynamically screened approximation*. However, the description ‘dynamically screened HF’ is a misnomer, since besides the screened HF exchange potential we also have a Coulomb hole contribution, as will be discussed shortly. The GWA has been very successful in describing bandstructures and bandgaps, as illustrated in figure 1 and table 1, kindly provided by Dr Eric Shirley.

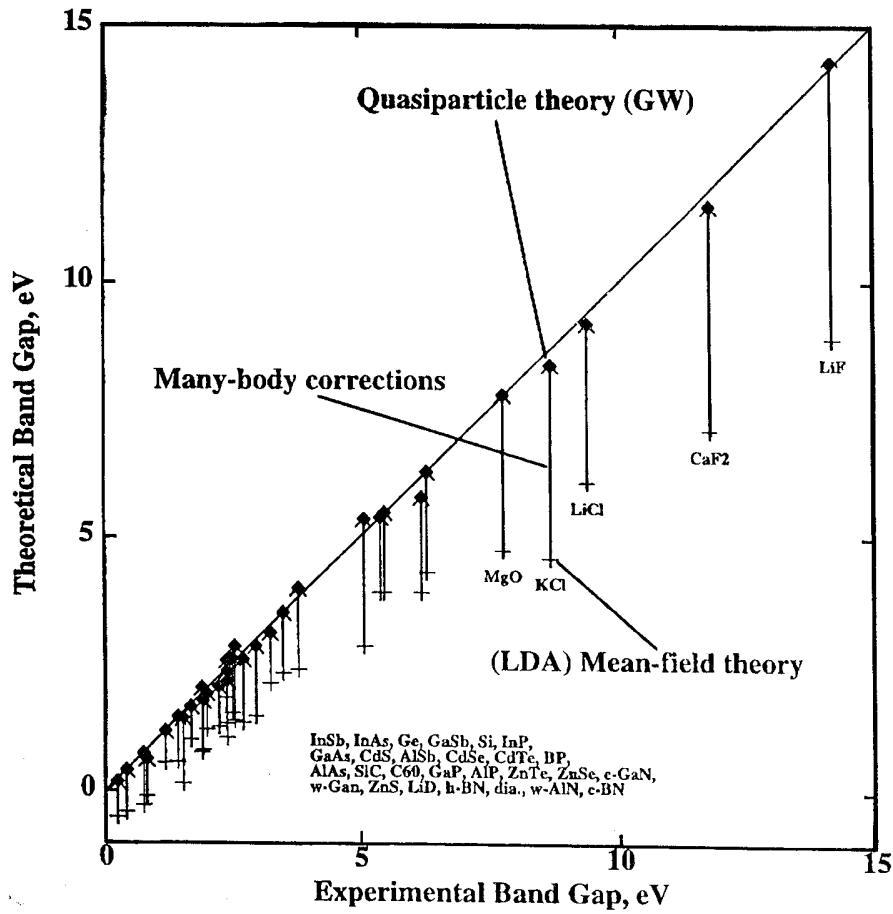


Figure 1. Results for bandgaps from the GWA and from the LDA. The straight line corresponds to perfect agreement with experiment. The data used in the figure are listed in table 1. The figure and the data were provided by Dr Eric Shirley, 1997.

Table 1. The data used in figure 1.

| LDA | GW | Experiment | Material | Reference | LDA | GW | Experiment | Material | Reference |
|-------|------|------------|------------------|-----------|-------|------|------------|----------|-----------|
| 3.9 | 5.5 | 5.48 | Diamond | [22–24] | 2.1 | 3.1 | 3.25 | cGaN | [33, 34] |
| 0.55 | 1.16 | 1.17 | Si | [22–24] | 2.3 | 3.5 | 3.5 | wGaN | [33, 34] |
| −0.27 | 0.73 | 0.74 | Ge | [24] | 1.82 | 2.55 | 2.39 | GaP | [31] |
| 1.31 | 2.34 | 2.39 | SiC | [23] | 0.15 | 1.42 | 1.52 | GaAs | [24] |
| 1.04 | 2.15 | 2.4 | Fullerite | [25] | −0.10 | 0.62 | 0.80 | GaSb | [21] |
| 8.91 | 4.31 | 4.2 | LiF | [26] | 3.9 | 5.8 | 6.2 | wAlN | [34] |
| 4.59 | 8.38 | 8.69 | KCl | [27] | 1.52 | 2.59 | 2.5 | AlP | [31] |
| 4.74 | 7.79 | 7.77 | MgO | [28, 29] | 1.25 | 2.03 | 2.23 | AlAs | [24] |
| 6.1 | 9.2 | 9.4 | LiCl | [21] | 1.00 | 1.64 | 1.68 | AlSb | [31] |
| 7.10 | 11.5 | 11.8 | CaF ₂ | [27] | 2.37 | 3.98 | 3.80 | ZnS | [34] |
| 1.2 | 1.9 | 2.0 | BP | [29] | 1.45 | 2.84 | 2.96 | ZnSe | [34] |
| 4.3 | 6.3 | 6.3 | cBN | [29] | 1.33 | 2.57 | 2.71 | ZnTe | [34] |
| 3.9 | 5.4 | 5.4 | hBN | [30] | 1.37 | 2.83 | 2.55 | CdS | [34] |
| 0.57 | 1.44 | 1.42 | InP | [31] | 0.76 | 2.01 | 1.90 | CdSe | [34] |
| −0.4 | 0.4 | 0.41 | InAs | [31] | 0.80 | 1.76 | 1.92 | CdTe | [34] |
| −0.5 | 0.18 | 0.23 | InSb | [31] | 2.84 | 5.37 | 5.09 | LiD | [27] |

The dynamically screened Coulomb potential can be expressed in *fluctuation potentials* (or oscillator strengths functions) $V^s(\mathbf{r})$:

$$W(\mathbf{r}, \mathbf{r}'; \omega) = \int \frac{\varepsilon^{-1}(\mathbf{r}, \mathbf{r}''; \omega)}{|\mathbf{r}'' - \mathbf{r}'|} d\mathbf{r}'' = \frac{1}{|\mathbf{r} - \mathbf{r}'|} + \sum_s \frac{2\omega_s V^s(\mathbf{r}) V^s(\mathbf{r}')}{\omega^2 - \omega_s^2}. \quad (14)$$

The precise definitions are

$$V^s(\mathbf{r}) = \int \frac{\rho^s(\mathbf{r}') d\mathbf{r}'}{|\mathbf{r} - \mathbf{r}'|} \quad \rho^s(\mathbf{r}) = \langle N, s | \rho_{op}(\mathbf{r}) | N \rangle \quad (15)$$

$$\rho_{op}(\mathbf{r}) = \int \psi^\dagger(x) \psi(x) d\xi \quad \omega_s = E(N, s) - E(N, 0) - i\delta.$$

When we have no magnetic fields we can choose the eigenfunctions, and thus also the $V^s(\mathbf{r})$, to be real. The bare Coulomb potential in equation (14) gives the Hartree–Fock exchange term V_{ex} . We define polarization contributions by

$$\Sigma_{GW} = V_{ex} + \Sigma_{pol} \quad W = v + W_{pol} \quad v(\mathbf{r}) = \frac{1}{|\mathbf{r}|}. \quad (16)$$

We define the matrix elements as

$$\langle kl | v | mn \rangle = \int \phi_k^*(x) \phi_l^*(x') v(\mathbf{r} - \mathbf{r}') \phi_m(x) \phi_n(x') dx dx'$$

$$V_{km}^s = \int \phi_k^*(x) V^s(\mathbf{r}) \phi_m(x) dx.$$

With these types of definition we have

$$\langle kl | W_{pol}(\omega) | k'l' \rangle = \sum_s \frac{2\omega_s V_{kk'}^s V_{ll'}^s}{\omega^2 - \omega_s^2}. \quad (17)$$

The integration in equation (13) can be carried out analytically, giving [35]

$$\Sigma_{pol}(x, x'; \omega) = \sum_{i,s \neq 0} \frac{V^s(\mathbf{r}) V^s(\mathbf{r}') \phi_i(x) \phi_i^*(x')}{\omega + \omega_s \operatorname{sgn}(\mu - \varepsilon_i) - \varepsilon_i}. \quad (18)$$

We replace G by G_0 and obtain for the matrix elements of Σ_{pol}

$$\langle k | \Sigma_{pol}(\omega) | l \rangle = \sum_{i,s \neq 0} \frac{V_{ki}^s V_{il}^s}{\omega + \omega_s \operatorname{sgn}(\mu - \varepsilon_i) - \varepsilon_i}. \quad (19)$$

The diagonal elements

$$\langle k | \Sigma_{pol}(\omega) | k \rangle = \sum_{i,s \neq 0} \frac{|V_{ki}^s|^2}{\omega + \omega_s \operatorname{sgn}(\mu - \varepsilon_i) - \varepsilon_i} \quad (20)$$

only contain contributions with positive weights, while the non-diagonal elements contain contributions with varying phases and will tend to cancel [16]. In a basis of HF orbitals we have, neglecting the non-diagonal terms, the QP energy expression

$$E_k = \varepsilon_k^{HF} + \langle k | \Sigma_{pol}(E_k) | k \rangle.$$

In many cases the LDA orbitals are close to the HF orbitals, and in a basis of LDA orbitals we can then make the approximation

$$E_k = \varepsilon_k^{LDA} + \langle k | \Sigma(E_k) - V_{xc} | k \rangle.$$

That the non-diagonal terms are small was recognized early [3]. In the following we will mainly discuss the diagonal elements of Σ .

The original derivation [1] took the GW approximation as the first term in an expansion of Σ in the full Green's function, G , and a screened potential from the exact linear response function, W . Actual calculations have however almost always used the unperturbed Green's function, G_0 , and an RPA screened potential, W_0 . Estimates of the effects of self-consistency, and of including higher-order terms, have only indicated small effects on quasi-particle energies, sometimes making them worse [3–5]. The effects on the shape of the spectral function are larger, but still small compared to the difference between the exact and the G_0W_0 results. This was demonstrated in a model calculation for the core-electron case, where the exact solution is known [35]. This topic is discussed in more detail in section 3.3.

When we use the approximation G_0W_0 it is not obvious how the energy scale for G_0 should be set. We allow for an arbitrary position by writing

$$G_0(x, x'; \omega) = \sum_i \frac{\phi_i(x) \phi_i^*(x')}{\omega - \varepsilon_i - \Delta E + i\delta \operatorname{sgn}(\varepsilon_i - \mu)} \quad (21)$$

where $\varepsilon_i = h_{ii}$. We then determine ΔE by demanding self-consistency at the Fermi surface:

$$E_k = \varepsilon_k + \langle k | \Sigma(E_k) | k \rangle = \varepsilon_k + \Delta E \quad k = k_F. \quad (22)$$

From equation (18) we have

$$\Sigma(\omega) = \Sigma^0(\omega - \Delta E)$$

where $\Sigma(\omega) = \Sigma_{G_0W_0}(\omega)$, $\Sigma^0(\omega) = \Sigma_{G_0^0W_0}(\omega)$, and $G_0^0 = G_0$ in equation (21) for $\Delta E = 0$. Equation (22) gives

$$\langle k_F | \Sigma^0(\varepsilon_{k_F}) | k_F \rangle = \Sigma_{k_F}^0(\varepsilon_{k_F}) = \Delta E.$$

In general we have

$$\begin{aligned} E_k &= \varepsilon_k + \Delta E + \Sigma_k^0(\varepsilon_k) - \Delta E + (E_k - \varepsilon_k - \Delta E) \frac{\partial \Sigma_k^0(\varepsilon_k)}{\partial \omega} + \dots \\ &\Rightarrow E_k = \varepsilon_k + \Delta E + Z_k [\Sigma_k^0(\varepsilon_k) - \Delta E] \end{aligned}$$

where

$$Z_k = \left[1 - \frac{\partial \Sigma_k^0(\varepsilon_k)}{\partial \omega} \right]^{-1}.$$

For the Green's function we have

$$G_k(\omega) = \frac{1}{\omega - \varepsilon_k - \Sigma_k(\omega)} = \frac{1}{\omega - \varepsilon_k - \Sigma_k^0(\omega - \Delta E)}. \quad (23)$$

3.2. The Coulomb hole plus screened exchange approximation; limiting cases

The non-diagonal matrix elements $\langle i|V_s|k\rangle$ of the fluctuation potential V_s approach zero as the energy difference $|\varepsilon_i - \varepsilon_k|$ increases. If this approach is fast enough, we can neglect the term $\varepsilon_k - \varepsilon_i$ in the denominator of the expression for $\langle k|\Sigma_{pol}(\varepsilon_k)|k\rangle$ in equation (20), which gives [36]

$$\begin{aligned} \langle k|\Sigma_{pol}(\varepsilon_k)|k\rangle &= \sum_{i,s \neq 0} \text{sgn}(\mu - \varepsilon_i) \frac{|V_{ki}^s|^2}{\omega_s} = 2 \sum_i^{occ} \sum_{s \neq 0} \frac{|V_{ki}^s|^2}{\omega_s} - \sum_i \sum_{s \neq 0} \frac{|V_{ki}^s|^2}{\omega_s} \\ &= - \sum_i^{occ} \langle ki|W_{pol}(0)|ik\rangle + \frac{1}{2} \sum_i \langle ki|W_{pol}(0)|ik\rangle. \end{aligned} \quad (24)$$

The first term combines with the HF exchange term to give a screened exchange (SEX) term:

$$- \sum_i^{occ} \langle ki|W(0)|ik\rangle.$$

The second term is called the Coulomb hole (COH) contribution:

$$\frac{1}{2} \int |\psi_k(\mathbf{r})|^2 W_{pol}(\mathbf{r}, \mathbf{r}; 0) \, d\mathbf{r}$$

since $W_{pol}(\mathbf{r}, \mathbf{r}; 0)$ is the Coulomb potential at the position \mathbf{r} from the charge pushed away by the presence of an electron at \mathbf{r} as obtained in linear response theory. The self-energy operator is connected with the energies required to add or remove an electron, and the factor 1/2 corresponds to doing so adiabatically.

As examples of how the COH–SEX approximation works, we first consider the removal of a *core electron* at the origin. In equation (24) k is a core state, and only the $i = k$ term gives a substantial contribution. Furthermore, the wavefunction $\psi_k(\mathbf{r})$ is strongly localized compared to the variation of $W_{pol}(\mathbf{r}, \mathbf{r}'; 0)$. In the localized limit we have

$$\langle k|\Sigma_{pol}(\varepsilon_k)|k\rangle = -\frac{1}{2} W_{pol}(\mathbf{0}, \mathbf{0}; 0). \quad (25)$$

Since $W_{pol}(\mathbf{0}, \mathbf{0}; 0)$ is a negative number, the core level is shifted upwards by the correlation effects. In this case it would clearly be an improvement to use a W from exact linear response theory rather than W_0 . A more accurate result is obtained if we calculate the adiabatic switch-on energy using non-linear response theory. However, the error from using a linear theory is quite small even though the energies themselves can easily be some 10 eV [37].

Next we consider highly excited *Rydberg states* of a free atom. We then consider an unoccupied state, and drop the screened exchange term in equation (24) to obtain

$$\langle k|\Sigma_{pol}(\varepsilon_k)|k\rangle = \frac{1}{2} \sum_i \langle ki|W_{pol}(0)|ik\rangle$$

which is the expectation value of

$$\Sigma_{pol}(x, x'; \omega) = \delta(x - x') \frac{1}{2} W_{pol}(\mathbf{r}, \mathbf{r}; 0).$$

A multipole expansion of W_{pol} to lowest order gives [1]

$$\Sigma_{pol}(x, x'; \omega) = -\delta(x - x') \frac{\alpha}{2r^4}$$

where α is the dipole polarizability. This well-known result can be obtained by a classical derivation [38]. Again it is an improvement if W is the exact rather than the RPA result.

Also the *image potential* on an electron outside a metal surface is reproduced. The screened exchange term in equation (24) can be dropped since the occupied wavefunctions decay exponentially outside the surface. In equation (25) $W_{pol}(\mathbf{r}, \mathbf{r}; 0)$ is the potential at \mathbf{r} from the charge pushed away in the solid by the presence of a point charge at \mathbf{r} . From classical electrodynamics we know that this is the image potential, i.e. we should have

$$W_{pol}(\mathbf{r}, \mathbf{r}; 0) = -\frac{1}{2z} \quad (26)$$

if the point \mathbf{r} is a distance z outside the solid. $W_{pol}(\mathbf{r}, \mathbf{r}; 0)$ gives this result already in the approximation for the dielectric function for a system with a surface, where the polarization function P , Fourier transformed with respect to the coordinates \mathbf{R} parallel to the surface, is taken as

$$P(\mathbf{Q}, z, z'; \omega) = \theta(z)\theta(z')[P_0(\mathbf{Q}, z - z'; \omega) + P_0(\mathbf{Q}, z + z'; \omega)] \quad (27)$$

with P_0 being the bulk system polarization function. This expression corresponds to specular electron reflection at the surface [39,40]. The screened potential corresponding to equation (27) can be obtained analytically (equation (26) in reference [41]), and equation (26) follows.

Now consider the correlation effects on a *bandgap*. For a state at the top of the valence band the largest contributions come from states i in the valence band, and the first (positive) term in equation (24) dominates. For a state at the bottom of the conduction band, on the other hand, we can drop the screened exchange term (we have an unoccupied state) and only keep the (negative) second term. Clearly, correlation effects make the bandgap smaller than its HF value [42].

Finally we consider an application not of the COH-SEX approximation but of the GWA itself, namely that to *electron energy loss*. The probability of decay per unit time of an electron in a state k in an electron gas is given by the imaginary part of the self-energy

$$w = \frac{2}{\hbar} |\text{Im} \Sigma(k, \varepsilon_k)| = \frac{2e^2}{\pi \hbar v} \int_0^\infty \frac{dq}{q} \int_0^{\omega_{\max}} \text{Im} \left[\frac{-1}{\varepsilon(q, \omega)} \right] d\omega \quad (28)$$

where

$$\hbar\omega_{\max}(k, q) = \text{Min} \left[\frac{\hbar^2}{2m} (2kq - q^2), \varepsilon_k - \varepsilon_F \right].$$

If we interpret equation (28) as a sum of probabilities for different energy losses $\hbar\omega$, we obtain the energy loss per unit time of the electron by inserting $\hbar\omega$ in the integral in equation (28) [43]:

$$\frac{dW}{dt} = \frac{2e^2}{\pi v} \int_0^\infty \frac{dq}{q} \int_0^{\omega_{\max}} \text{Im} \left[\frac{-\omega}{\varepsilon(q, \omega)} \right] d\omega.$$

Almost the same expression is obtained from linear response theory by taking the electron as an external particle moving on a straight trajectory and calculating the work done on the system. The only difference is that ω_{\max} is replaced by $\hbar kq/m = vq$. This replacement makes little difference except close to the Fermi surface.

It should be remarked that while the COH-SEX approximation gives a qualitatively correct picture of the basic physics, it is often quantitatively not so accurate. In cases where we study electrons which can be more or less considered as classical charges, like core levels and Rydberg states, it works very well however. The COH-SEX approximation is considerably improved if a short-ranged part is taken out first, as shown by Gygi and Baldereschi [44, 45].

3.3. Comments on the RPA, r_s -expansions, and vertex corrections

The acronym RPA was used for the random-phase approximation in the Bohm–Pines theory of 1953 for an electron gas [46]. In 1957 it was shown by Hubbard [47] that the Bohm–Pines theory gives similar results to the diagrammatic bubble expansion for the dielectric function, which in turn was shown by Ehrenreich and Cohen [48] in 1959 to be equivalent to the time-dependent Hartree approximation (THA), or the Lindhard approximation [49] from 1954. The developments of the Bohm–Pines theory are tailor-made for an electron gas, and not easily generalizable to say an atom or a solid, while the THA is completely general. Despite this, the RPA is used synonymously with the THA and with bubble expansion. More serious, however, is that the RPA is often associated with the 1957 Gell-Mann and Brueckner [50] small- r_s expansion of the bubble diagrams, an expansion that is very poor for metallic densities, while the THA on the other hand gives meaningful results at metallic densities also.

The background for this unfortunate association has to do with the celebrated success of the Gell-Mann and Brueckner theory [50] for the electron gas correlation energy. Then it was indeed a big achievement to identify the bubble diagrams as the most divergent terms in the diagram expansion, and to show that their sum gave a finite result, and the dominating correlation contribution at high electron densities. That the bubble series gives useful results when evaluated exactly (as shown by Hubbard) and not as an r_s -expansion has surprisingly not yet fully eradicated the Gell-Mann and Brueckner picture in which the bubble diagrams are poor at metallic densities. Part of the reason for this is that Hubbard stressed the comparatively small difference between the Pines results for the electron gas correlation energy and the bubble series result, rather than the much larger difference between the exact bubble (or THA) and the bubble r_s -expansion results, the latter being wrong in the metallic region. Quinn and Ferrell [51] in a well-known paper from 1958 gave the GW expression for Σ , but did not recognize its usefulness beyond the case of an electron gas, and only evaluated the results as an r_s -expansion. Even in a work as late as 1962 by Quinn [43] on the range of excited electrons in metals, where the result was calculated with the RPA dielectric function, the estimate of its range of validity was based on the DuBois [52] 1959 discussion of the r_s -expansion.

To improve the THA, Hubbard went beyond the Hartree approximation by taking exchange effects into account. This leads us to look more closely at different possibilities for evaluating the GWA. To simplify the discussion, we limit ourselves here to the electron gas problem. We then have the exact relations

$$\begin{aligned} G(k) &= \frac{1}{\varepsilon - \varepsilon_k - \Sigma(k)} & \Sigma(k) &= i \int \frac{d^4q}{(2\pi)^4} G(k-q)W(q)\Lambda(k, q) \\ W(q) &= \frac{v(q)}{\varepsilon(q)} & v(q) &= \frac{4\pi}{|q|^2} & \varepsilon(q) &= 1 - v(q)P(q) \\ P(q) &= -2i \int \frac{d^4q}{(2\pi)^4} G(k-q)G(k)\Lambda(k, q) & \Lambda(k, q) &= 1 + \frac{\delta\Sigma(k)}{\delta V_C(q)} \end{aligned}$$

where V_C is the total Coulomb potential from the electron ground-state density and from external sources. We have used the notation $k = (\mathbf{k}, \varepsilon)$, and suppressed the spin variables. Clearly, the GWA comes from taking the *vertex function* $\Lambda(k, q) = 1$, i.e. neglecting the variation in the self-energy when the Coulomb potential varies. Almost all calculations have used G_0W_0 instead of GW , where W_0 is taken from the RPA—schematically, $P = P_0 = G_0G_0$. We will refer to this as the RPA case.

A fully self-consistent calculation with

$$G = (\varepsilon - \varepsilon_k - \Sigma)^{-1} \quad \Sigma = GW \quad W = v(1 - vGG)^{-1}$$

was carried out by Holm and von Barth [53], and by Schöne and Egiluz [54]. The results are very poor for the satellite region of the spectral function $A(\omega)$. The reason for this is that the self-consistent W turned out to be very far from the correct W , resulting in an almost complete smoothing of the satellite structure. Also the QPs were affected, and the agreement with experiment became worse than with G_0W_0 . A partially self-consistent calculation with $W = v(1 - vG_0G_0)^{-1}$, and only G made self-consistent, gave more reasonable results [55,56]. Most quantities underwent only small changes. The satellite was reduced and moved closer to the QP peak, which is the correct trend, but the movement was not large enough. These results for conduction electrons are in agreement with results from a similar model study of the core-electron problem [35], where the *exact* solution is known.

The effects of vertex corrections, i.e. of going from GW to $GW\Lambda$, were discussed by Mahan [57]. Mahan, as well as Del Sole, Reining, and Godby [58], and Hindgren and Almladh [59], mainly discussed *local* vertex corrections. One then obtains

$$\Lambda(q) = \frac{1}{1 + vgP_0} \quad W = W_1 \equiv \frac{(1 + vgP_0)v}{1 - v(1 - g)P_0} \quad G = G_0$$

and thus

$$\Sigma = G_0W_2 \quad W_2 = \frac{v}{1 - v(1 - g)P_0}. \quad (29)$$

Here g is the local field factor frequently discussed in the literature. The first suggestion for g came from Hubbard [47]:

$$g(q) = \frac{1}{2} \frac{q^2}{q^2 + k_s^2}.$$

In the LDA, g is strictly quadratic in q , $g(q) = -(dv_{xc}/dn)/v(q)$, instead of correctly flattening out as in Hubbard's expression. The effective screened potential W_2 is the LDA result for the screening potential acting on an electron from a test charge, while W_1 is the screening potential acting on a test charge from a test charge [60]. There are many calculations using equation (29) and they all give very similar results for the QP energies. Strong support for the G_0W_2 form was given by Rice [61]. He showed that a functional derivative of the total energy for an electron gas with respect to the electron occupation number, and using Hubbard's energy expression corrected for exchange effects [47], gave a QP energy corresponding to G_0W_2 .

To summarize the rather complex topic of self-consistency and vertices, we have found that the G_0W_0 (RPA) approximation is consistently reasonable. Attempts to improve on it have to be made very carefully, and one can easily obtain completely distorted results. In practice, W is usually calculated using a THA expression but with LDA wavefunctions, sometimes including local field factors, i.e. a TLD approximation (time-dependent LDA). TLDA calculations recommend themselves since they have given very good phonon properties [18], and also good plasmon dispersions in metals [62].

The limiting cases for G_0W_0 which we have discussed pertain to situations not connected with the high-density limit, and still give results known to be correct. Mild changes of G_0W_0 like shifting the QP energies in G_0 and using a local field factor in W , like in W_2 , lead to improvements. If we consider G_0W_0 as the first term in a perturbation expansion, we have to proceed with utmost care when we try to estimate corrections, a situation not uncommon in perturbation theory. An interesting possibility as regards applying perturbation theory to Σ on the basis of DFT has been presented by Farid [6].

4. Electron–boson model Hamiltonians and fluctuation potentials

4.1. Introduction

The G_0W_0 approximation has been very successful in giving good QP energies, but the results for the spectral function have important shortcomings. This had already become clear with the work by Langreth in 1970 [63] on core-electron photoemission in a metal where plasmon excitations dominate. Following Lundqvist's work from 1967 [64], Langreth studied a polaron model:

$$H = \varepsilon_c c^\dagger c + c c^\dagger \sum_q g_q (a_q + a_q^\dagger) + \sum_q \omega_q a_q^\dagger a_q. \quad (30)$$

Here c^\dagger creates a core electron of energy ε_c , and a_q^\dagger a plasmon of energy ω_q . The coupling coefficient is

$$g_q = \sqrt{v(q)\omega_p^2/(2\omega_q)} \quad (31)$$

where ω_p is the plasmon energy. This model allows an exact solution for the spectral function, which can be compared with the GW result, and with perturbation expansions starting with the GW term. The seemingly simple core-electron model Hamiltonian in equation (30) is actually quite realistic as we will discuss in the next subsection.

Lundqvist [64] showed that the G_0W_0 approximation for an electron gas can be regarded as the second-order perturbation result from a polaron model Hamiltonian similar to that in equation (30). An interesting discussion of such a Hamiltonian was also given by Overhauser in 1971 [65].

We introduce a model Hamiltonian, applicable not only for core electrons or the electron gas but also for a general situation (atoms, molecules, and solids):

$$H = H_0 + V$$

where

$$H_0 = \sum_k \varepsilon_k c_k^\dagger c_k + \sum_s \omega_s a_s^\dagger a_s \quad V = \sum_{s k k'} V_{k k'}^s (a_s + a_s^\dagger) c_k^\dagger c_{k'}. \quad (32)$$

To lowest order, the self-energy is (cf. e.g. Migdal's work on electron–phonon couplings, reference [66])

$$\Sigma_{kl}(\omega) = \frac{i}{2\pi} \sum_{k's} \int G_{k'}(\omega - \omega') V_{k k'}^s D_s(\omega') V_{k'l}^s d\omega' \quad (33)$$

with

$$G_k(\omega) = \frac{1}{\omega - \varepsilon_k} \quad D_s(\omega) = \frac{2\omega_s}{\omega^2 - \omega_s^2}.$$

Equation (33) is identical to the polarization part of the GWA, equation (19), provided that the coupling functions $V_{k k'}^s$ in equation (32) are identified with the fluctuation potentials in equation (15).

In this section we will argue that the relevance of the model Hamiltonian in equation (32) goes beyond its use in second-order perturbation theory. Its relevance for the core-electron case was clearly demonstrated by Langreth [63], and is further elaborated on in section 4.2, and its relevance for valence electrons is argued in section 4.3. The model is physically appealing; it describes an *electronic polaron* with an electron coupled to density fluctuations described as effective bosons. The model also allows us to make approximations useful for photoemission and other spectroscopies like electron scattering [9]. For photoemission we

show in section 5.2 how the high-energy limit corresponds to the coupling of the photoelectron to density fluctuations. The idea of an electronic polaron has a long history; an interesting discussion and a historical review can be found in the paper by Fowler [67].

It is difficult to directly evaluate the fluctuation potentials, since they are defined in terms of interacting many-body states. If we on the other hand use a RPA or THA response it is not guaranteed that the screened potential can be written in a spectral resolution form as in equation (14), which allows the identification of the potentials $V^s(\mathbf{r})$. In the RPA it can anyway be shown that [14]

$$V^s(\mathbf{r}) = \int W(\mathbf{r}, \mathbf{r}'; \omega_s) \tilde{\phi}_s(\mathbf{r}') d\mathbf{r}' \quad (34)$$

where $\omega_s = \varepsilon_k - \varepsilon_l$ ($\varepsilon_k > \mu > \varepsilon_l$) and $\tilde{\phi}_s(\mathbf{r}) = \phi_k(\mathbf{r})\phi_l(\mathbf{r})$, i.e. the state s corresponds to a particle-hole excitation. For the electron gas in the RPA there are no particle-hole pairs in the energy region where we find the plasmons. In such a case there are additional fluctuation potentials. They are obtained by solving the eigenvalue problem $(1 - vP(\omega))w_i = \lambda_i(\omega)w_i$ for a given ω , and then finding the root ω_i from $\lambda_i(\omega_{im}) = 0$. The fluctuation potential is

$$V^{im}(\mathbf{r}) = \left| \frac{\partial \lambda_i(\omega)}{\partial \omega} \right|^{-1/2} w_i(\mathbf{r}; \omega) \Big|_{\omega=\omega_{im}}. \quad (35)$$

In the electron gas case, i stands for the momentum \mathbf{q} of a bulk plasmon excitation, and there is only one root m for each \mathbf{q} . The bulk plasmons are extended excitations where the wavefunctions are modified by the surface, but not their energies. The surface plasmons on the other hand are localized in the direction perpendicular to the surface. They are hence characterized only by the momentum \mathbf{K} parallel to the surface, while the perpendicular momentum is undetermined. A surface plasmon of momentum \mathbf{K} is degenerate with electron-hole pairs of parallel momentum \mathbf{K} , and a perpendicular momentum to give the pair the same energy as the surface plasmon. A bulk plasmon of momentum \mathbf{q} has on the other hand no degenerate electron-hole pairs of momentum \mathbf{q} until $|\mathbf{q}|$ is larger than a cut-off momentum k_c (in the RPA). Thus the surface plasmon eigenvalues of $\lambda_i(\omega_{im}) = 0$ are complex, and the surface plasmons are accounted for by equation (34), as are the bulk plasmons for $|\mathbf{q}| > k_c$.

4.2. The core-electron spectrum

Equation (30) is a special case of equation (32) with only one fermion level, i.e. the labels \mathbf{k} and \mathbf{k}' are replaced by single label c . The boson labels s stand for plasmon momenta \mathbf{q} and we have $V_{\mathbf{k}\mathbf{k}'}^s = g_q \delta_{\mathbf{k},c} \delta_{\mathbf{k}',c} \delta_{s,q}$. From equation (33) we have

$$\Sigma_c^0(\omega) = \frac{i}{2\pi} \sum_q g_q^2 \int G_c^0(\omega - \omega') D_q(\omega') d\omega' = \int \frac{\beta(\omega') d\omega'}{\omega + \omega' - \varepsilon_c} \quad (36)$$

with

$$\beta(\omega) = \sum_q g_q^2 \delta(\omega - \omega_q) = \frac{1}{\pi} \left(\frac{r_s^3}{12} \right)^{1/4} \frac{\omega_p^2}{\omega} \sqrt{\frac{\omega_p}{\omega - \omega_p}} \theta(\omega - \omega_p) \quad (37)$$

where we have used the simple plasmon dispersion $\omega_q = \omega_p + q^2/2$ [20]. From equation (36) we have

$$\text{Im} \Sigma_c^0(\omega) = \pi \beta(\varepsilon_c - \omega) \quad \beta(\omega) = \frac{1}{\pi} \text{Im} \Sigma_c^0(\varepsilon_c - \omega). \quad (38)$$

The GWA spectral function is (cf. equation (23))

$$A_c(\omega) = \frac{1}{\pi} \frac{\text{Im} \Sigma_c^0(\omega - \Delta E)}{(\omega - \varepsilon_c - \text{Re} \Sigma_c^0(\omega - \Delta E))^2 + (\text{Im} \Sigma_c^0(\omega - \Delta E))^2} \\ = \frac{\beta(E_c - \omega)}{(\omega - \varepsilon_c - \text{Re} \Sigma_c^0(\omega - \Delta E))^2 + \pi^2 \beta^2(E_c - \omega)}.$$

$A_c(\omega)$ has a broad satellite peak starting at $\omega = \varepsilon_c - \omega_p$ and extending to $\omega = -\infty$. At the QP energy $\text{Im} \Sigma_c^0$ is infinitesimal and $A_c(\omega)$ has a peak, $\delta(\omega - \varepsilon_c - \text{Re} \Sigma_c^0(\omega - \Delta E))$. The QP energy E_c follows from $E_c - \varepsilon_c - \text{Re} \Sigma_c^0(E_c - \Delta E) = 0$, i.e. $E_c = \varepsilon_c + \Delta E$, where

$$\Delta E = \text{Re} \Sigma_c^0(\varepsilon_c) = \int \frac{\beta(\omega) d\omega}{\omega}.$$

The strength of the QP peak is

$$Z^{GW} = \frac{1}{1 - \partial \text{Re} \Sigma_c^0(\omega - \Delta E) / \partial \omega} \Big|_{\omega=E_c} = \left[1 + \int \frac{\beta(\omega)}{\omega^2} d\omega \right]^{-1}.$$

The spectral function corresponding to the simple model Hamiltonian in equation (30) can be calculated exactly by a canonical transformation which removes the linear term in the boson operators [63]. With this Hamiltonian, the core-electron Green's function is

$$G_c(t) = i \langle \Psi_0 | c^\dagger e^{i(H-E_0)t} c | \Psi_0 \rangle \theta(-t). \tag{39}$$

The core-electron terms can easily be eliminated, giving

$$G_c(t) = i e^{-i\varepsilon_c t} \theta(-t) \sum_n e^{iE_n^* t} |\langle n^* | 0 \rangle|^2 \tag{40}$$

where $|0\rangle$ is the ground state of the Hamiltonian

$$H_{bos} = \sum_q \omega_q a_q^\dagger a_q$$

and $|n^*\rangle$ is an eigenstate of H_{bos}^* with energy E_n^* :

$$H_{bos}^* = H_{bos} + \sum_q g_q (a_q + a_q^\dagger) = \sum_q \left[\omega_q \tilde{a}_q^\dagger \tilde{a}_q - \frac{g_q^2}{\omega_q} \right] \quad \tilde{a}_q = a_q - \frac{g_q}{\omega_q}.$$

Using the relation between the eigenstates $|n^*\rangle$ of H_{bos}^* and $|n\rangle$ of H_{bos} , we obtain

$$|n\rangle = e^{-S} |n^*\rangle \quad S = \sum_q \frac{g_q}{\omega_q} (a_q^\dagger - a_q). \tag{41}$$

Some algebra gives

$$\sum_n e^{iE_n^* t} |\langle n^* | 0 \rangle|^2 = \exp \left\{ -i \Delta E t + \sum_q \frac{g_q^2}{\omega_q^2} (e^{i\omega_q t} - 1) \right\} \quad \Delta E = \sum_q \frac{g_q^2}{\omega_q}. \tag{42}$$

To obtain $G_c(\omega)$ and $A_c(\omega)$, we Fourier transform $G_c(t)$ to obtain

$$G_c(\omega) = i \int_{-\infty}^0 e^{i(\omega - \varepsilon_c - \Delta E)t} \exp \left\{ \sum_q \frac{g_q^2}{\omega_q^2} (e^{i\omega_q t} - 1) \right\} dt.$$

With $E_c = \varepsilon_c + \Delta E$ and

$$Z = \exp \left\{ - \sum_q \frac{g_q^2}{\omega_q^2} \right\}$$

and making a Taylor expansion of the exponent we have

$$G_c(\omega) = iZ \int_{-\infty}^0 e^{i(\omega-E_c)t} \exp\left\{\sum_q \frac{g_q^2}{\omega_q^2} e^{i\omega_q t}\right\} dt$$

$$= Z \left\{ \frac{1}{\omega - E_c} + \sum_q \frac{g_q^2}{\omega_q^2} \frac{1}{\omega - E_c + \omega_q} + \dots \right\}.$$

This exact solution for $G_c(\omega)$ gives a spectral function

$$A_c = (1/\pi) \text{Im } G_c(\omega)$$

(cf. equation (37)):

$$A_c(\omega) = Z \left[\delta(\omega - E_c) + \frac{\beta(E_c - \omega)}{(\omega - E_c)^2} + \dots \right]$$

which has a QP peak of strength Z plus a series of satellites, the first starting at $\omega = E_c - \omega_p$, the second starting at $\omega = E_c - 2\omega_p$, etc. The GWA result is

$$A_c^{GW}(\omega) = Z^{GW} \delta(\omega - E_c) + \frac{\beta(E_c - \omega)}{(\omega - \varepsilon_c - \text{Re } \Sigma_c^0(\omega - \Delta E))^2 + \pi^2 \beta^2 (E_c - \omega)}. \tag{43}$$

Remarkably the QP energies are identical, and the Z -values are fairly similar—namely, $Z^{GW} = [1 + \bar{n}]^{-1}$ as compared to $Z = e^{-\bar{n}}$, where

$$\bar{n} = \sum_q g_q^2 / \omega_q^2 = \int \beta(\omega) / \omega^2 d\omega. \tag{44}$$

The quantity \bar{n} is the mean number of shake-up plasmons and has the value $\bar{n} = 0.201r_s^{3/4}$ in our simple plasmon model [20]. In the metallic density region when r_s varies from say $r_s = 2$ (for Al) to $r_s = 4$ (for Na), \bar{n} goes from 0.34 to 0.57, and Z from 0.71 to 0.57. The strength in the satellite structure is substantial; it varies from 0.29 to 0.43 (the spectral function A is normalized to 1). The weakly correlated ‘simple’ metals thus actually have substantial correlation effects!

While the QP energy comes out exactly and the QP strength is reasonable in the GWA, the satellite structure consists of only one peak instead of a series of peaks; see figure 2. The

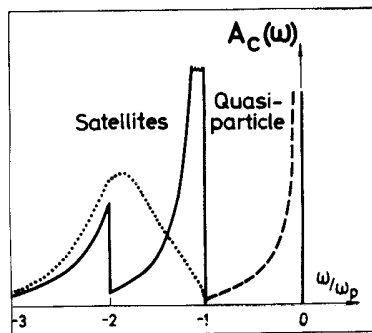


Figure 2. Comparison of the first order or the GWA (dotted line) and the exact (full line) results for the core-electron spectral function as obtained from the model Hamiltonian in equation (30). In this model the quasi-particle peak is a delta function. The dashed curve indicates a more realistic form of the QP peak. The results are for $r_s = 4$. From reference [68].

centre of gravity of the spectrum remains at the unshifted core-electron energy

$$\int \omega A_c(\omega) d\omega = \varepsilon_c$$

both in the GWA and in the exact solution [20].

When the correlation effects are small, i.e. when β is small, then A_c^{GW} agrees with A_c . The high density of states for plasmons at small q -values causes β to have a square-root singularity at the onset of the satellite structure, and the β^2 -term in the denominator of A_c^{GW} shifts the satellite peak from $E_c - \omega_p$ to something more like $E_c - 2\omega_p$. With the built-in limitation of the GWA that there is only one satellite peak, this peak actually represents the many-peak structure of the exact solution fairly well (figure 2).

From equation (39) for $G_c(t)$, we can obtain $A_c(\omega)$ as

$$\begin{aligned} A_c(\omega) &= \frac{1}{\pi} \text{Im} \langle \Psi_0 | c^\dagger \frac{1}{\omega + H - E_0 - i\delta} c | \Psi_0 \rangle \\ &= \langle \Psi_0 | c^\dagger \delta(\omega + H - E_0) c | \Psi_0 \rangle = \sum_n |\langle n^* | 0 \rangle|^2 \delta(\omega + E_n^* - E_0). \end{aligned} \quad (45)$$

Using equation (42) we find the following expression for $A_c(\omega)$ ($E_0 = \varepsilon_c$):

$$A_c(\omega) = \frac{1}{2\pi} \int_{-\infty}^{\infty} dt e^{i(\omega - \varepsilon_c)t} \exp \left\{ \int \beta(\omega') \frac{(e^{i\omega't} - i\omega't - 1)}{(\omega')^2} d\omega' \right\} \quad (46)$$

which turns out to be valid also for the much more general Hamiltonian (see references [63] and [20])

$$H = H_v + \varepsilon_c c^\dagger c + V c c^\dagger \quad (47)$$

provided that $\beta(\omega)$ is properly defined. Here the core electrons still enter in a simple way, and we still only need to consider two valence-electron Hamiltonians, one when the core-electron level is occupied, H_v , and one when it is empty, $H_v + V$. H_v includes all inter-electron interactions, while V is an attractive one-electron potential between the core hole and the valence electrons:

$$V = \sum_{i=1}^N w(\mathbf{r}_i).$$

If we neglect the usually small valence–core exchange term, then

$$w(\mathbf{r}) = - \int |\mathbf{r} - \mathbf{r}'|^{-1} \rho_c(\mathbf{r}') d\mathbf{r}'$$

and if we use pseudopotentials, $w(\mathbf{r})$ is the difference between the (unscreened) potentials of an ion with a core hole and one without. The exact strength function $\beta(\omega)$ can be expanded in powers of w , the lowest-order term being

$$\beta(\omega) = \sum_s |W_s(\mathbf{0})|^2 \delta(\omega - \omega_s) \quad (48)$$

where $W_s(\mathbf{r})$ is

$$W_s(\mathbf{r}) = \int w(\mathbf{r}) \rho_s(\mathbf{r}) d\mathbf{r}.$$

This result is a simple reformulation of equation (146) in reference [20] using the fluctuation density $\rho_s(\mathbf{r})$, defined in equation (15). To make contact with the electron gas case that we just discussed, we use the plasmon-fluctuation potential in equation (35) ($i = q$):

$$V_q = \sqrt{v_q \omega_p^2 / (2\omega_q)} \exp(i\mathbf{q} \cdot \mathbf{r})$$

which allows us to extract

$$\rho_q = \sqrt{\omega_p^2 / (2v_q \omega_q)} \exp(iq \cdot r)$$

and W_q :

$$W_q(r) = \sqrt{\frac{w_q^2 \omega_p^2}{2v_q \omega_q}} e^{iq \cdot r}$$

If we further take the core-electron charge density $\rho_c(r)$ as a delta function, and use a bare Coulomb potential in the expression for $w(r)$, we reproduce equations (31) and (37).

Our results show that for the calculation of the core-electron spectral function to $O(w^2)$ in an exponential (cumulant) expression on the level of approximation given in equation (47), we can use the electron–boson model Hamiltonian in equation (32) with $W_s(r)$ instead of $V_s(r)$. If we do not use pseudopotentials and neglect valence–core exchange, the two potentials are equal, $W_s(r) = V_s(r)$ (cf. reference [20]). In particular, our results show that the electron–hole pairs described by the fluctuation potential in equation (34) can be included, and will produce the MND singular QP line shape (MND stands for Mahan–Nozieres–de Dominicis, see [69], section 8.3 D). The core-electron satellites are thus given by an exponential expression which looks very different from the GW expression, or improvements of it via low-order expansions in W .

Expanding to second order in W , we have [35]

$$\begin{aligned} \Sigma(\varepsilon) = & \int_0^\infty G(\varepsilon + \omega) \beta(\omega) d\omega \\ & + \int_0^\infty \int_0^\infty G(\varepsilon + \omega) G(\varepsilon + \omega + \omega') G(\varepsilon + \omega') \beta(\omega) \beta(\omega') d\omega d\omega' \end{aligned} \quad (49)$$

where $G(\omega) = [\omega - \Sigma(\omega)]^{-1}$, and $\beta(\omega)$ is the function given in equation (37), which is proportional to $\text{Im } W$. We see that equation (49) reduces to equation (36) (with $\varepsilon_c = 0$) if we keep only the first term in equation (49), and replace $G(\omega) = [\omega - \Sigma(\omega)]^{-1}$ by $G_0(\omega) = \omega^{-1}$. The exact result for the spectral function $A(\omega) = (1/\pi) \text{Im } G(\omega)$ is compared with that from $G_0 W_0$ in figure 3, with that from GW_0 using only the first term (self-consistently) in equation (49) in figure 4, and with that from $GW_0 GW_0 G$ using both terms (self-consistently) in equation (49) in figure 5. Clearly, going from $G_0 W_0$ to GW_0 makes only a slight change, while going to second order in W_0 gives a fairly good result. We have used a model β -function with the fairly small asymmetry index of 0.1. The higher satellites are not shown in the figures. These results indicate that a (self-consistent) expansion in W_0 may work. Computationally, such an expansion is however much more difficult to handle than the exponential expression.

4.3. Valence-electron spectra

The exponential expressions (48), (46) for the core-electron case can also be obtained by summing the diagrams where we have only one fermion line dressed by all possible emissions and reabsorptions of bosons; see figure 6. It is then reasonable to also approximate the valence-electron Green’s function by summing the same set of diagrams. The summation however cannot be done exactly, since the electrons recoil when emitting or absorbing a boson, which mixes Green’s functions with different momenta, and thus also mixes electrons and holes. One can obtain an approximation for the valence-hole Green’s function in the same spirit as for the core-hole one by:

- (a) Neglecting processes where the hole is converted to an electron, i.e. always taking

$$n_{p+q_1+q_2+\dots} = 1.$$

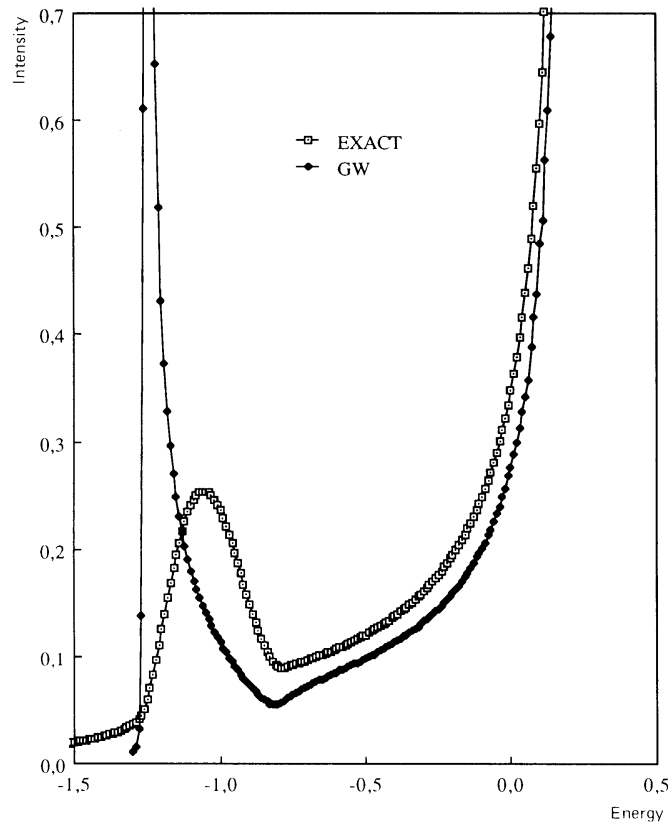


Figure 3. Comparison between the GWA as obtained from the first term in equation (49), and the exact solution for a model core-electron spectrum. Only the first plasmon satellite is shown. From reference [35].

(b) Replacing the multiparticle recoil denominator:

$$\varepsilon_{p+q_1+q_2+\dots} + \omega_{q_1} + \omega_{q_2} + \dots \rightarrow \varepsilon_p + \sum_i (\varepsilon_{p+q_i} - \varepsilon_p + \omega_{q_i}).$$

The valence-electron diagram series is then identical to the core diagram series, except that the boson dispersion is changed from ω_q to $\varepsilon_{p+q} - \varepsilon_p + \omega_q$. Condition (b) means that all $q_i q_j$ -terms are neglected compared to the p^2 - and $p q_i$ -terms. These approximations give a β_k -function to use in equation (46), which is formally similar to the core-electron one; cf. equation (38):

$$\beta_k(\omega) = \frac{1}{\pi} \text{Im} \Sigma(\mathbf{k}, \varepsilon_k - \omega) \theta(\mu - \varepsilon_k + \omega). \quad (50)$$

Since $\text{Im} \Sigma$ has a sharp onset of the plasmon structure, equation (50) will give a set of plasmon peaks much as for the core-electron case.

Approximation (b) was used by McMullen and Bergersen [70] in 1974 in discussing high-energy electrons, where it is certainly justified. The possibility of using approximations (a) and (b) for hole propagation in metals and plasmon losses was discussed in reference [7]. In particular, it was found that they should apply for small \mathbf{k} and high electron densities,

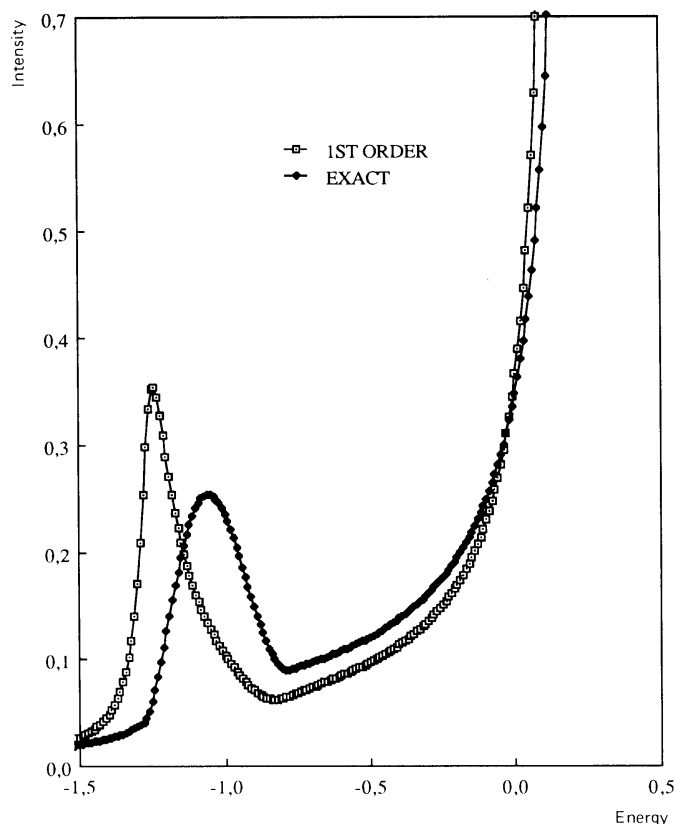


Figure 4. Comparison between the self-consistent result obtained using the first term in equation (49), and the exact solution for a model core-electron spectrum. Only the first plasmon satellite is shown. From reference [35].

thus establishing that it was possible to have a series of plasmon losses in the valence-electron case also. The same result was obtained by Almladh and Hedin [20] without using diagram expansions by iterating the equation of motion for $G(\mathbf{k}, t)$ starting from $G^0(\mathbf{k}, t) = i \exp(-iE_k t) \theta(-t)$. This was also obtained in reference [71] from a cumulant expansion. The cumulant treatment has the advantage of being more streamlined, and allowing higher-order terms to be calculated in a straightforward way. The contributions beyond the lowest order discussed here are however cumbersome to handle; there were 656 terms in the next order which were evaluated by a computer program. The calculations in reference [71] were for a different problem to that considered here, where the couplings are much stronger than in metals; the mean number of bosons \bar{n} was 1 or larger. Still, the indications are that the first-order term gives a reasonable approximation. The electronic polaron model probably should not be taken beyond the lowest-order diagram since the bosons are assumed to represent all screened interactions and the next order includes terms with an electron-hole bubble, which represents double counting. Also higher-order exchange diagrams are missing in the polaron model. Early discussions of an exponential expression were given by Doniach in 1970 [72] and by Müller-Hartmann, Ramakrishnan, and Toulouse [73] who investigated the threshold singularity. In reference [73] there was also a discussion of the representation of particle-hole excitations by effective bosons.

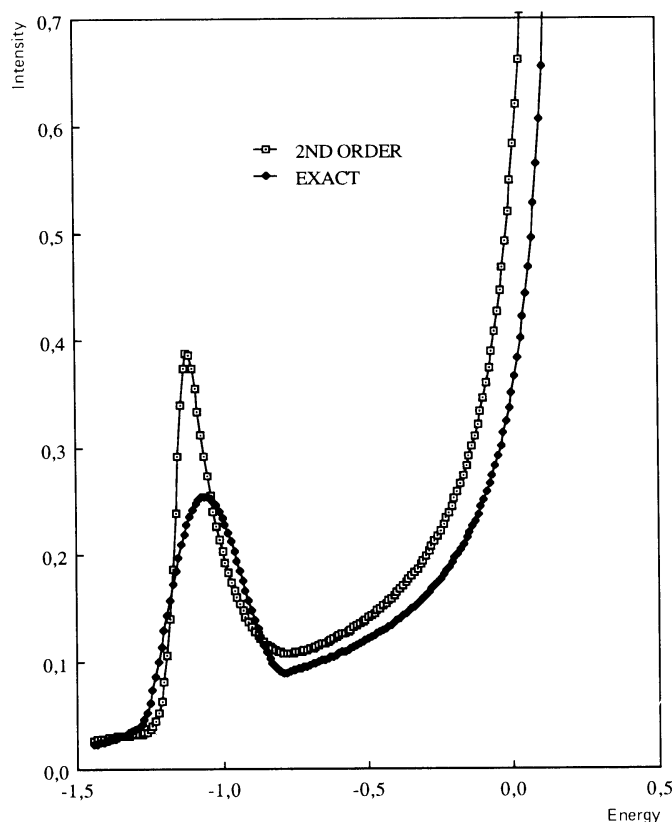


Figure 5. Comparison between the self-consistent result obtained using both terms in equation (49), and the exact solution for a model core-electron spectrum. Only the first plasmon satellite is shown. From reference [35].

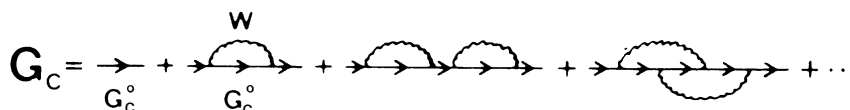


Figure 6. The diagram expansion for the core-electron Green's function. From reference [7].

In a recent work [10] the exponential expression was evaluated for some real systems using *a priori* bandstructure calculations, and it was also shown that the satellite structure is closely related to the electron energy-loss function. In figure 7 the spectral function for Na metal obtained from the exponential expression is compared with the *GW* result for $\mathbf{k} = (2\pi/a)[1, 1, 1/2]$. We note the large displacement to smaller binding energies of the *GW* satellite peak, and the structure in the satellite peak due to bandstructure effects. Experimental results clearly favour a satellite structure much closer to the exponential than to the *GWA* results. It is also clear, both from numerical results in reference [10] and from analytic model calculations in reference [7] that the QP line shape is barely changed when going from the *GWA* to the exponential expression.

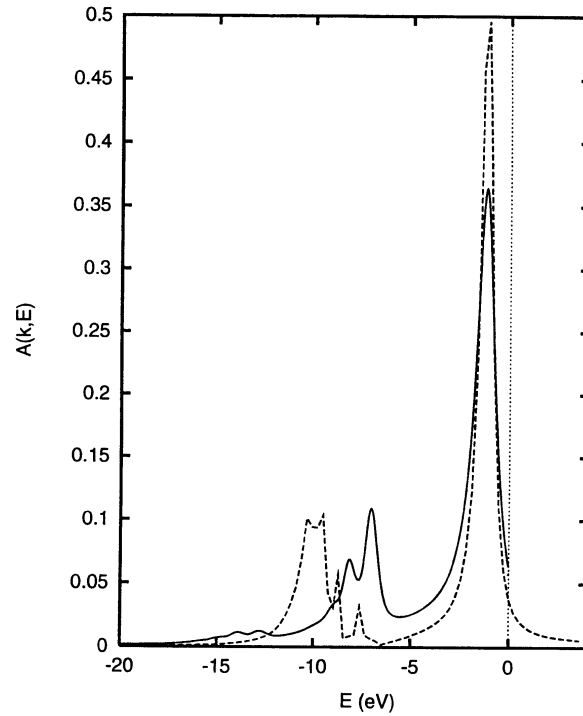


Figure 7. The spectral function for Na with $k = (2\pi/a)[1, 1, 1/2]$. The solid and dashed lines correspond to the cumulant expansion and the GWA respectively. From reference [10].

5. Photoemission theory beyond the sudden approximation

5.1. General aspects

In equation (10) we give the general expression for the photocurrent. The exact final state is however not the sudden approximation $c_k^\dagger |N-1, s\rangle$ given in equation (11), but

$$|N-1, s; \mathbf{k}\rangle = \left[1 + \frac{1}{E - H - i\eta} (H - E) \right] c_k^\dagger |N-1, s\rangle. \quad (51)$$

The additional term includes the processes in which the photoelectron scatters on its way out of the solid. The first description of this effect was given by Berglund and Spicer in 1964 [74]. They argued that photoemission was a three-step process: (1) photoexcitation; (2) transport to the surface, and (3) passage through the surface. In steps (2) and (3) the electron could scatter and lose energy. If the photoexcitation created an energy distribution $A(\omega)$, the photocurrent should simply be the convolution of $A(\omega)$ with the loss probabilities from steps (2) and (3). This description is certainly correct at high enough electron energies. The problem is that most measurements are made at energies where the electron mean free path is only say 5–20 Å. Equation (51) shows that we have to add amplitudes for the direct process (the one in the sudden approximation) and the loss process, and we expect quantum interferences. To analyse this problem we will use the electron–boson model Hamiltonian in equation (32), and we will limit ourselves to core-electron photoemission. We will also discuss why it is reasonable to use this Hamiltonian for photoemission by analysing the high-energy limit. First however we give a few elementary comments.

The final state $|N - 1, s; \mathbf{k}\rangle$ is an eigenstate of the full Hamiltonian H including the couplings between the photoelectron and the solid. We may think of the sudden approximation state $c_{\mathbf{k}}^{\dagger}|N - 1, s\rangle$ as an eigenstate of some Hamiltonian H_0 where these couplings are left out. Due to the identity of the photoelectron and the electrons in the target, we cannot however write down an explicit form for H_0 . If we make approximations such that we can write $H = H_0 + V$, where $c_{\mathbf{k}}^{\dagger}|N - 1, s\rangle$ is an eigenfunction of H_0 with eigenvalue E , then we can replace $H - E$ in equation (51) by V to obtain the usual Lippmann–Schwinger expression. The final states $|N - 1, s; \mathbf{k}\rangle$ in the photoemission problem are the same as in electron scattering except for time inversion. Thus a scattering process with an incoming electron \mathbf{k} , and a set of scattered electrons \mathbf{k}' , on time inversion has incoming waves $-\mathbf{k}'$ and one outgoing wave $-\mathbf{k}$. In core-electron photoemission the state $c_{\mathbf{k}}^{\dagger}|N - 1, s\rangle$ has a photoelectron \mathbf{k} , plus a core hole, and some excitations of the valence electrons described by the index s . The Berglund–Spicer primary energy distribution $A_c(\omega)$ comes from resolving the initial state for the valence electrons $|0\rangle$ into eigenstates $|n^*\rangle$ of the Hamiltonian with a core hole; cf. equation (40). One talks about *shake-up* or *intrinsic losses*, as compared to the *extrinsic losses* of the electron on its way out. For threshold photon energy there are no losses; by energy conservation we must have a zero-energy photoelectron, and the solid in its ground state. At very high energies the extrinsic scattering rates go to zero, but at the same time the mean free path goes to infinity. The result is that the intensity ratio of the electrons in the satellite relative to that in the main QP peak goes to a constant value. In the high-energy limit the intrinsic and extrinsic contributions to the ratio are additive, being 1 for the extrinsic and $1 - Z$ for the intrinsic parts. The sudden approximation gives a current proportional to the volume of the solid, which of course is unphysical. Even if we divide out the volume factor, the relative intensities are wrong at any photon energy. The reason that the spectral function is commonly used to interpret photoemission experiments is the interest in QP energies, where the photon energy dependence of the satellite structure does not matter. If however we are interested in the satellite structure—it is crucial e.g. for strongly correlated systems—or in line shapes of QPs, we must go beyond the one-electron spectral function.

5.2. Photoemission in the high-energy limit and fluctuation potentials

In the high-energy limit we can rewrite the photoemission expression to identify a potential V which couples the photoelectron to the electrons in the solid, and we find that the coupling functions are fluctuation potentials. This leads us to introduce the model Hamiltonian in equation (32) to describe the photoemission process. Our presentation here builds on appendix A in reference [14].

Chew and Low [75] observed that one could write the final state as

$$|N - 1, s; \mathbf{k}\rangle = c_{\mathbf{k}}^{\dagger}|N - 1, s\rangle + \frac{1}{E - H - i\eta} V_{CL}|N - 1, s\rangle$$

where

$$V_{CL} = [H, c_{\mathbf{k}}^{\dagger}] - \epsilon_{\mathbf{k}} c_{\mathbf{k}}^{\dagger}.$$

Evaluating the commutator we have

$$[H, c_{\mathbf{k}}^{\dagger}] = \sum_{\mathbf{k}_1} c_{\mathbf{k}_1}^{\dagger} h_{\mathbf{k}_1 \mathbf{k}}^0 + \frac{1}{2} \sum_{\mathbf{k}_1 \mathbf{k}_2 \mathbf{k}_3} \langle \mathbf{k}_1 \mathbf{k}_2 || v || \mathbf{k} \mathbf{k}_3 \rangle c_{\mathbf{k}_1}^{\dagger} c_{\mathbf{k}_2}^{\dagger} c_{\mathbf{k}_3}$$

where $h^0 = -\nabla^2/2 + V_{nucl}$ and where $\langle \mathbf{k}_1 \mathbf{k}_2 || v || \mathbf{k} \mathbf{k}_3 \rangle$ is an antisymmetrized Coulomb matrix element. We add and subtract a term

$$\sum_{\mathbf{k}_1 \mathbf{k}_2 \mathbf{k}_3} c_{\mathbf{k}_1}^{\dagger} \langle \mathbf{k}_1 \mathbf{k}_2 || v || \mathbf{k} \mathbf{k}_3 \rangle \langle N - 1, s | c_{\mathbf{k}_2}^{\dagger} c_{\mathbf{k}_3} | N - 1, s \rangle$$

and choose the one-electron basis to diagonalize the HF-like one-electron Hamiltonian

$$h_{\mathbf{k}_1\mathbf{k}}^0 + \sum_{\mathbf{k}_2\mathbf{k}_3} \langle \mathbf{k}_1\mathbf{k}_2 || v || \mathbf{k}\mathbf{k}_3 \rangle \langle N-1, s | c_{\mathbf{k}_2}^\dagger c_{\mathbf{k}_3} | N-1, s \rangle.$$

We consider a finite solid, and the continuum states are thus scattering states with free-electron energies ϵ_k . The $\epsilon_k c_k^\dagger$ terms in V_{CL} then cancel, and we have

$$V_{CL} = \sum_{\mathbf{k}_1\mathbf{k}_2\mathbf{k}_3} c_{\mathbf{k}_1}^\dagger \langle \mathbf{k}_1\mathbf{k}_2 || v || \mathbf{k}\mathbf{k}_3 \rangle \left(\frac{1}{2} c_{\mathbf{k}_2}^\dagger c_{\mathbf{k}_3} - \langle N-1, s | c_{\mathbf{k}_2}^\dagger c_{\mathbf{k}_3} | N-1, s \rangle \right).$$

We now discuss which the dominating terms are when the photoelectron has a high energy.

In the last term the states \mathbf{k}_2 and \mathbf{k}_3 must have limited energies, since the state $|N-1, s\rangle$ has a limited range of virtual one-electron energies. Furthermore, \mathbf{k}_1 must have a large energy; otherwise the matrix element $\langle \mathbf{k}_1\mathbf{k}_2 || v || \mathbf{k}\mathbf{k}_3 \rangle$ becomes small.

In the first term $c_{\mathbf{k}_3}$ must have a limited energy since it works on $|N-1, s\rangle$. Thus one of \mathbf{k}_1 and \mathbf{k}_2 must have a limited energy, and one a high energy (since \mathbf{k} has a high energy); otherwise the matrix element $\langle \mathbf{k}_1\mathbf{k}_2 || v || \mathbf{k}\mathbf{k}_3 \rangle$ becomes small. The first term is symmetric in \mathbf{k}_1 and \mathbf{k}_2 , and we can thus choose \mathbf{k}_1 to have a high energy, and omit the factor 1/2.

We denote states with a high energy by \mathbf{k} and with a limited energy by l , and have

$$V_{CL} \approx \sum_{\mathbf{k}_1 l_1 l_2} c_{\mathbf{k}_1}^\dagger \langle \mathbf{k}_1 l_1 || v || \mathbf{k} l_2 \rangle (c_{l_1}^\dagger c_{l_2} - \langle N-1, s | c_{l_1}^\dagger c_{l_2} | N-1, s \rangle).$$

Again utilizing the properties of the Coulomb matrix elements, we can write (where we have dropped the small exchange part in the antisymmetrized Coulomb matrix element)

$$|N-1, s; \mathbf{k}\rangle = \left[1 + \frac{1}{E - H - i\eta} V \right] c_{\mathbf{k}}^\dagger |N-1, s\rangle \quad (52)$$

where

$$V = \sum_{\mathbf{k}_1\mathbf{k}_2} \sum_{l_1 l_2}^{fast\ slow} c_{\mathbf{k}_1}^\dagger c_{\mathbf{k}_2} \langle \mathbf{k}_1 l_1 || v || \mathbf{k}_2 l_2 \rangle [c_{l_1}^\dagger c_{l_2} - \langle N-1, s | c_{l_1}^\dagger c_{l_2} | N-1, s \rangle]. \quad (53)$$

We can write V in terms of the density operator

$$\rho(\mathbf{r}) = \sum_{l_1 l_2} \psi_{l_1}^*(\mathbf{r}) \psi_{l_2}(\mathbf{r}) c_{l_1}^\dagger c_{l_2}$$

and have

$$V = \sum_{\mathbf{k}_1\mathbf{k}_2} c_{\mathbf{k}_1}^\dagger c_{\mathbf{k}_2} \int \psi_{\mathbf{k}_1}^*(\mathbf{r}) v(\mathbf{r} - \mathbf{r}') (\rho(\mathbf{r}') - \langle \rho(\mathbf{r}') \rangle) \psi_{\mathbf{k}_2}(\mathbf{r}) \mathbf{d}\mathbf{r} \mathbf{d}\mathbf{r}'. \quad (54)$$

We now have the expected result: *at high energies we can treat the photoelectron as a distinguishable particle interacting with the density fluctuations of the target system.*

We will now simplify the full Hamiltonian by omitting terms which do not contribute to the photocurrent in the high-energy limit. First we divide the one-electron states into l -states, which are sufficient to describe the correlations of the many-body states $|N-1, s\rangle$, and the remaining states, the k -states. Only k -states in a limited energy range below the maximum possible photoelectron k -value will enter. We can drop terms containing Coulomb interactions with one or three k -states, since the Coulomb integrals involved are small. We can also drop Coulomb interactions with four k -states since they do not contribute when H operates on $V c_{\mathbf{k}}^\dagger |N-1, s\rangle$. The only Coulomb terms left are

$$V = \sum_{\mathbf{k}_1\mathbf{k}_2} \sum_{l_1 l_2} \langle \mathbf{k}_1 l_1 || v || \mathbf{k}_2 l_2 \rangle c_{\mathbf{k}_1}^\dagger c_{\mathbf{k}_2} c_{l_1}^\dagger c_{l_2}.$$

This leaves us with a Hamiltonian

$$H = H_s + h + V \tag{55}$$

where H_s describes the solid with all of the electron–electron interactions (only l -states), $h = h^0 + V^{HF}$ describes the photoelectron (only k -states), and V (equation (54)) is the interaction between the photoelectron and the solid. Thus in a perturbation expansion of equation (52) we can work with eigenstates of $H_s + h$, which form a product basis, $|s'\rangle|\mathbf{k}'\rangle$, where for simplicity we have written $|s'\rangle$ for $|N - 1, s'\rangle$. The interaction V can then be written as

$$V = \sum_{\mathbf{k}_1 \mathbf{k}_2} \sum_{s_1 s_2} \int \langle \mathbf{k}_1 | V^{s_1 s_2} | \mathbf{k}_2 \rangle |s_1\rangle \langle s_2 | c_{\mathbf{k}_1}^\dagger c_{\mathbf{k}_2}$$

where

$$V^{s_1 s_2}(\mathbf{r}) = \int v(\mathbf{r} - \mathbf{r}') \langle s_1 | \rho(\mathbf{r}') - \langle \rho(\mathbf{r}') | s_2 \rangle d\mathbf{r}'. \tag{56}$$

In an extended system we may think of an excited state $|s'\rangle$ as having a finite number of extended boson-type excitations. Since each boson excitation only changes the charge density by a term proportional to (volume)⁻¹, we take $\langle s' | \rho(\mathbf{r}) | s' \rangle = \langle 0 | \rho(\mathbf{r}) | 0 \rangle$, for all s' . In a one-electron theory the charge-density operator $\rho(\mathbf{r})$ creates electron–hole pairs, and $\langle s' | \rho(\mathbf{r}) | s'' \rangle$ is then different from zero only when the state s' contains one more or one less electron–hole pair, say t , than we have in s'' . With a finite number of pairs we can replace $\langle s' | \rho(\mathbf{r}) | s'' \rangle$ by $\langle t | \rho(\mathbf{r}) | 0 \rangle$ or $\langle 0 | \rho(\mathbf{r}) | t \rangle$. The charge fluctuations $\langle t | \rho(\mathbf{r}) | 0 \rangle$ determine the charge-fluctuation potentials; equation (15). We represent $|s_1\rangle \langle s_2|$ by a_s^\dagger when s_1 has one boson s more than s_2 , and by a_s when it has one less, and H_s by a boson Hamiltonian. With these approximations we arrive at the model Hamiltonian H in equation (32). We note that all bosons and couplings refer to the final state.

5.3. Core-electron photoemission in metals

The presentation in this subsection builds on the work in reference [14]. With our model Hamiltonian in equation (32) we can write the photoemission current as

$$J_{\mathbf{k}}(\omega) = \sum_s |\tau_s(\mathbf{k})|^2 \delta\left(\omega - \varepsilon_{\mathbf{k}} - \sum_\nu \omega_\nu n_\nu(s)\right) \tag{57}$$

with

$$\tau_s(\mathbf{k}) = \langle N - 1, s | c_{\mathbf{k}} \left[1 + V \frac{1}{E - H + i\eta} \right] \sum_{ij} \Delta_{ij} c_i^\dagger c_j | N, 0 \rangle. \tag{58}$$

We have shifted the energy scale for ω to remove the large core-electron binding energy ε_c , such that the maximum energy of the photoelectron is ω . The index s specifies the occupation number $n_\nu(s)$ for the boson ν . The operator c_j in equation (58) annihilates the core electron c . The core electrons are then out of the picture. Going over to a product representation for the eigenstates of H_0 in equation (32), we have

$$\tau_s(\mathbf{k}) = \langle \mathbf{k} | \langle s^* | \left[1 + V \frac{1}{E - H + i\eta} \right] | 0 \rangle \sum_{\mathbf{k}'}^{unocc} |\mathbf{k}'\rangle \langle \mathbf{k}' | \Delta | c \rangle \tag{59}$$

where $|0\rangle$ is the ground state for the valence electrons in the initial state, i.e. with no core hole present, and $|s^*\rangle$ is an eigenstate for the valence electrons in the final state, i.e. with a core hole present. We have specified the label i as \mathbf{k}' . Neglecting the restriction ‘unocc’ on the sum

$\sum_{\mathbf{k}'}^{unocc} |\mathbf{k}'\rangle\langle\mathbf{k}'|$, which is exact for higher photoelectron energies, we can replace it by a delta function, and have the compact expression

$$\tau_s(\mathbf{k}) = \langle\mathbf{k}|\langle s^*| \left[1 + V \frac{1}{E - H + i\eta} \right] |0\rangle\Delta|c\rangle = \tau_s^1(\mathbf{k}) + \tau_s^2(\mathbf{k}).$$

Here $\tau_s^1(\mathbf{k}) = \langle\mathbf{k}|\Delta|c\rangle\langle s^*|0\rangle$ is the sudden-approximation result that we discussed earlier. In particular we noticed that it was unrealistic since it gave a current proportional to the volume of the system. One expects the state $|\mathbf{k}\rangle$ to be damped inside the solid giving a current proportional to the radiated surface area. This effect plus the effects from extrinsic scattering must come from the $\tau_s^2(\mathbf{k})$ term.

To obtain the damped photoelectron states we carry out a partial summation in V using Feshbach's projection operator technique [76] with $P = |s^*\rangle\langle s^*|$ and $Q = 1 - P$, which gives [8, 14]

$$\tau_s(\mathbf{k}) = \langle\tilde{\mathbf{k}}|\langle s^*| \left[1 + V \frac{1}{E - QHQ + i\eta} \right] |0\rangle\Delta|c\rangle$$

where

$$\langle\tilde{\mathbf{k}}| = \langle\mathbf{k}| \frac{i\eta}{\varepsilon_{\mathbf{k}} - h - P\Sigma P + i\eta} \quad P\Sigma P = PV \frac{1}{E - QHQ + i\eta} VP$$

and $\langle\tilde{\mathbf{k}}|$ is the damped state. Using the transformation operator S defined by equation (41), we arrive at the compact result

$$\tau_s(\mathbf{k}) = \langle\tilde{\mathbf{k}}|T_s\Delta|c\rangle \quad T_s = \langle s^*| \left[1 + V \frac{1}{E - QHQ + i\eta} \right] e^{-S}|0^*\rangle. \quad (60)$$

Comparing with equation (45), we find that it agrees, apart from the dipole matrix element, when we put $V = 0$.

The lowest-order result obtained from these equations for a final state having one boson ν is

$$T_\nu = V^\nu G(\varepsilon_{\mathbf{k}} + \omega_\nu) - \frac{V_{cc}^\nu}{\omega_\nu} \quad (61)$$

where

$$G(\omega) = \frac{1}{\omega - h - \Sigma(\omega)} \quad \Sigma(\mathbf{r}, \mathbf{r}'; \omega) = \sum_\nu V^\nu(\mathbf{r}) \frac{1}{\omega - h - \omega_\nu + i\eta} V^\nu(\mathbf{r}').$$

The self-energy Σ is the particle part in the GW expression; i.e. its imaginary part is the same when $\omega > \mu$, but the real part is slightly different.

As a simple model for estimating the energy variation of the photocurrent, we consider a semi-infinite jellium with the surface in the xy -plane and an atom embedded at a distance z_c from the surface. By symmetry, the fluctuation potentials then have the form

$$V^\nu(\mathbf{r}) = e^{i\mathbf{Q}_\nu \cdot \mathbf{R}} V^\nu(z)$$

where $\mathbf{R} = (x, y)$ and \mathbf{Q}_ν is the momentum parallel to the surface. We take the dipole matrix element as varying slowly with \mathbf{k} , and can then omit it since we are interested in relative intensities. Doing the algebra, we have

$$|\tau_\nu(\mathbf{k})| = e^{-z_c \text{Im} \tilde{\mathbf{k}} - \tilde{n}/2} h_\nu \quad (62)$$

where

$$h_\nu = \left| \int f(z) V^\nu(z) dz \right| \quad f(z) = \frac{\delta(z - z_c)}{\omega - \varepsilon_{\mathbf{k}}} + \frac{i}{\kappa} e^{i(\tilde{\mathbf{k}} - \kappa)(z - z_c)} \theta(z_c - z) \quad (63)$$

where

$$\tilde{k} = \sqrt{k^2 + 2(\phi + i\Gamma(\epsilon_k))} \quad \kappa = \sqrt{2(\omega + \phi + i\Gamma(\omega)) - |\mathbf{Q}_v + \mathbf{K}|^2}.$$

The photoelectron wavevector is $\mathbf{k} = (\mathbf{K}, k)$ and $\phi > 0$ is the workfunction, while \bar{n} is defined in equation (44). The first term in f in equation (63) comes from the intrinsic process, and the second from extrinsic scattering. The potential $V^v(z)$ is essentially a surface-modified plane wave for the extended fluctuation potentials, i.e. those from bulk plasmons and particle-hole pairs. For the surface plasmons, when they are regarded as stable, the function $V^v(z)$ is localized at the surface. The expression for the one-boson contribution to the photocurrent is

$$J_{\mathbf{k}}(\omega) = e^{-2z_c \text{Im} \tilde{k} - \bar{n}} \gamma(\omega - \epsilon_k) \quad \gamma(\omega) = \sum_v h_v^2 \delta(\omega - \omega_v). \quad (64)$$

Since $J_{\mathbf{k}}(\omega)$ is quadratic in V^v , the photocurrent, to lowest order, can be written in terms of $\text{Im} W$ (cf. equation (14)):

$$J_{\mathbf{k}}(\omega) = \frac{-1}{\pi} e^{-2z_c \text{Im} \tilde{k} - \bar{n}} \sum_{\mathbf{Q}} \int f(z) f(z')^* \text{Im} W(\mathbf{Q}, z, z'; \omega - \epsilon_k) dz dz'. \quad (65)$$

We can write an exponential expression which in lowest order reproduces the photocurrent from equation (64), and picks up all terms with zero and one extrinsic contribution in the expansion of equation (60):

$$J_{\mathbf{k}}(\omega) = \frac{1}{2\pi} \int_{-\infty}^{\infty} e^{i(\omega - \epsilon_k)t} \exp \left[\int \gamma(\omega)(e^{-i\omega t} - 1) d\omega \right] dt. \quad (66)$$

Expanding the exponential, we have

$$J_{\mathbf{k}}(\omega) = \exp \left(- \int \gamma(\omega) d\omega \right) [\delta(\omega - \epsilon_k) + \gamma(\omega - \epsilon_k)]. \quad (67)$$

Equation (67) agrees with equation (64), provided that

$$\int \gamma(\omega) d\omega = 2z_c \text{Im} \tilde{k} + \bar{n}.$$

This relation was checked analytically in the high-energy limit, and also numerically. The expansion of the exponent in equation (66) converges nicely if the boson energies have a minimum value—say ω_0 . The first-order (one-boson) contribution then starts at ω_0 below the QP, the second order at $2\omega_0$ below, etc. Equation (64) is however divergent for electron-hole contributions, while equation (66) is well defined and correctly gives the pure intrinsic spectrum in equation (46) (except for the $i\omega t$ term; cf. reference [77]). The intrinsic part (the first term in f) clearly dominates over the extrinsic part (the second term in f) at threshold ($\epsilon_k \rightarrow \omega$).

The quantum mechanical (QM) result in equation (66) can be compared to the Berglund–Spicer (BS) result, and to the semi-classical (SC) one. In the SC case we calculate the probabilities of excitation in the valence-electron system from a classical charge moving with velocity v , the time-dependent perturbing potential (for an electron moving perpendicular to the surface) being [14]

$$V^v(t) = \int V^v(\mathbf{r}) \rho(\mathbf{r}, t) d\mathbf{r} \quad \rho(\mathbf{r}, t) = [\delta(z + vt - z_c) - \delta(z - z_c)] \delta(\mathbf{R}) \theta(t). \quad (68)$$

In all three cases the photocurrent takes the same form as in equation (66), but with different γ -functions. We have

$$\gamma^{QM}(\omega) = \sum_v h_v^2 \delta(\omega - \omega_v) \quad (69)$$

$$h_v = \left| \frac{V^v(z_c)}{\omega_v} + \frac{i}{\kappa} \int_{-\infty}^{z_c} \exp[i(\tilde{k} - \kappa)(z - z_c)] V^v(z) dz \right|$$

$$\gamma^{BS}(\omega) = \frac{\alpha(\omega)}{\omega} + z_c \tau(\varepsilon, \omega) \quad (70)$$

$$\alpha(\omega) = \sum_v \frac{V_v^2}{\omega_v} \delta(\omega - \omega_v)$$

$$\gamma^{SC}(\omega) = \sum_v \tilde{h}_v^2 \delta(\omega - \omega_v) \quad (71)$$

$$\tilde{h}_v = \left| \frac{V^v(z_c)}{\omega_v} + \frac{i}{v} \int_{-\infty}^{z_c} \exp\left[\frac{-i\omega_v(z - z_c)}{v}\right] V^v(z) dz \right|.$$

In equation (70) $\tau(\varepsilon, \omega)$ is the differential inverse mean free path (see e.g. reference [78]), where ε is the electron energy (kept constant) and ω the energy loss. The results from the three approximations for the first plasmon satellite are given in figure 8. We see that the QM and SC results approach each other fairly quickly, and above say 3–4 au the difference is insignificant, while at low energies like 2 au there are substantial differences. The BS result, on the other hand, is grossly off up to very high energies of the order of keV. We note the two peaks in the BS curves at lower energies. They arise from the intrinsic losses, which start at the threshold energy ω_p , and the extrinsic losses, which start at a slightly higher energy determined by momentum/energy selection rules. It should also be noted that how the fluctuation potential is approximated makes a large impact. In figure 9 we compare results obtained using a fluctuation potential that goes smoothly to zero at the surface [8] and one that is a plane wave combined with a step function [79].

In figure 10 we show results for the first bulk plasmon satellite with and without the interference term in the transition amplitude [8]. Thus if we write $\tau_v = \tau_v^{intr} + \tau_v^{extr}$, figure 10 shows results for $|\tau_v^{intr} + \tau_v^{extr}|^2$ and $|\tau_v^{intr}|^2 + |\tau_v^{extr}|^2$. To understand the trends, we use the Inglesfield fluctuation potential [80]:

$$V^v(\mathbf{r}) = A_v e^{iQ_v \cdot \mathbf{r}} [\cos(q_v z + \phi_v) - \cos \phi_v e^{-Q_v z}] \theta(z) \quad A_v = \sqrt{\frac{4\pi\omega_p^2}{(Q_v^2 + q_v^2)\omega_v}} \quad (72)$$

and write equations (60) and (61) more explicitly:

$$\tau_v(\mathbf{k}) = \frac{\langle \mathbf{k} | V^v | \mathbf{k} + \mathbf{q} \rangle}{\varepsilon_{\mathbf{k}} + \omega_v - \varepsilon_{\mathbf{k}+\mathbf{q}}} \langle \mathbf{k} + \mathbf{q} | \Delta | c \rangle - \frac{V_{cc}^v}{\omega_v} \langle \mathbf{k} | \Delta | c \rangle$$

where for simplicity we have omitted the tilde symbols on the momenta, and skipped the self-energy in G . At threshold for the satellite, the $\mathbf{q} = 0$ plasmons are involved. We then have

$$\tilde{\tau}_v(\mathbf{k}) = [\langle \mathbf{k} | V^v | \mathbf{k} \rangle - V_{cc}^v] \frac{\langle \mathbf{k} | \Delta | c \rangle}{\omega_v}.$$

For a pure bulk potential, $V^v(\mathbf{r}) = 2^{-1/2} A_v \exp(i\mathbf{q} \cdot \mathbf{r})$, which makes $[\langle \mathbf{k} | V^v | \mathbf{k} \rangle - V_{cc}^v] = 0$, i.e. there is perfect destructive interference between the intrinsic and extrinsic terms. When ω_v and q_v increase, the recoil makes the difference between intrinsic and extrinsic terms larger, and this goes faster for larger values of \mathbf{k} . Also the cancellation is more effective the further away from the surface z_c is. These two trends are more or less visible in the figures. The cancellation effects are easy to understand from the semi-classical approximation. When v approaches zero the two delta functions in equation (68) cancel, or, as expressed by Gadzuk [81], the long-wavelength plasmons are excited by the average potential from the core hole plus the photoelectron, which is zero. An estimate of the range of strong cancellations, based on the phase velocity, has been given by Inglesfield [80].

In figure 11 we show the integrated satellite intensities relative to that in the main peak for the QM and SC cases. The curves rapidly approach each other with increasing energy, and are already close at say 5 au, while they approach the BS value (indicated by the dashed

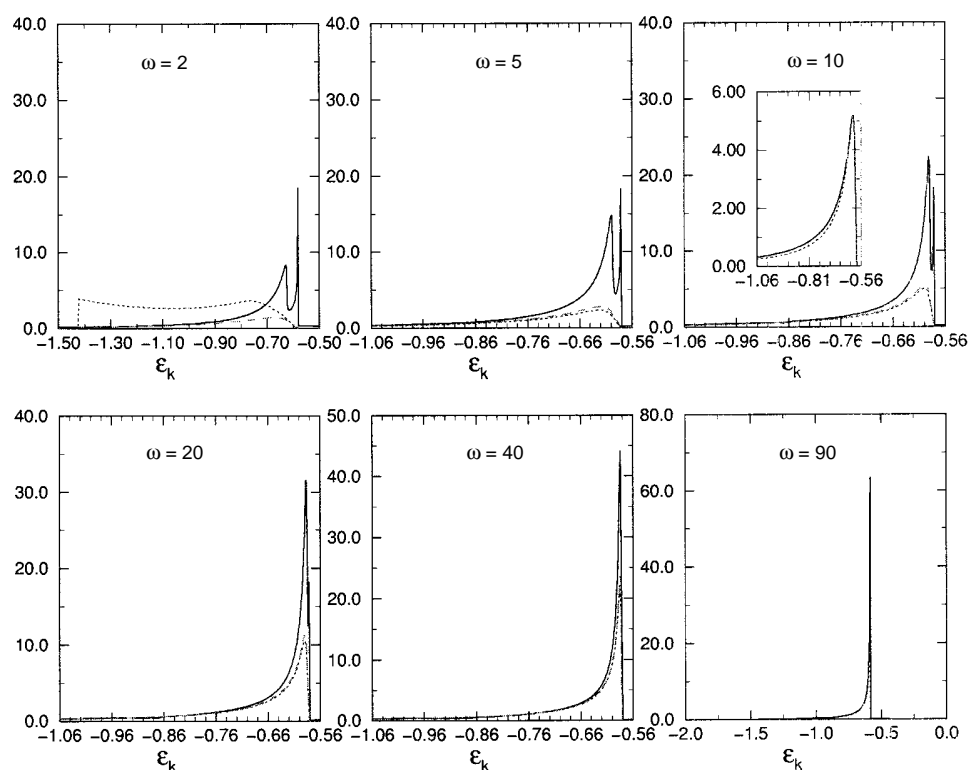


Figure 8. Bulk plasmon satellite spectra for various photon energies ω , and integrated over the position of the core hole. The convolution result proposed by Berglund and Spicer [74] (BS) is indicated by a solid line, the quantum mechanical theory (QM) presented here by a dotted line, and the semi-classical (SC) result, obtained from putting the photoelectron on a trajectory, by a dashed line. The inset for $\omega = 10$ compares results obtained with two different fluctuation potentials, one given by Inglesfield (solid curve) and the other by Bechstedt *et al* (dotted curve). The photoelectron energies are with respect to the quasi-particle position. From reference [14].

line) quite slowly, following the $(\epsilon_k)^{-1/2}$ dependence derived by Chang and Langreth [83]. At lower energies, the QM curve has a pronounced maximum. This is due to the damping of the QP electrons being stronger than that of the electrons in the satellite, when the QP electron has an energy on the sharply rising part of the $\Gamma(\omega)$ curve, $\Gamma(\omega)$ being the QP width. The sharp rise comes from the onset of plasmon damping. This effect does not arise in the SC approximation, where the damping has to be put in by hand, and is the same for the elastic peak and the satellites.

Results which were obtained including particle-hole pairs are shown in figures 12 and 13. In figure 12 the energy is 5 au, and the core distance 20 au. Only the surface plasmon contribution is included. The different contributions to the total spectrum—the intrinsic, the extrinsic, and the interference parts—are shown separately. We see that out to say 2 eV the intrinsic part dominates. At the surface plasmon peak the extrinsic and interference parts are large and cancel strongly. We also see that interference effects are important only in a narrow region at the peak of the surface plasmon, and in particular they are very small in the quasi-particle tail. Since the intrinsic contribution dominates at threshold, we can obtain an energy-independent singularity index α by fitting our numerical results to a power law,

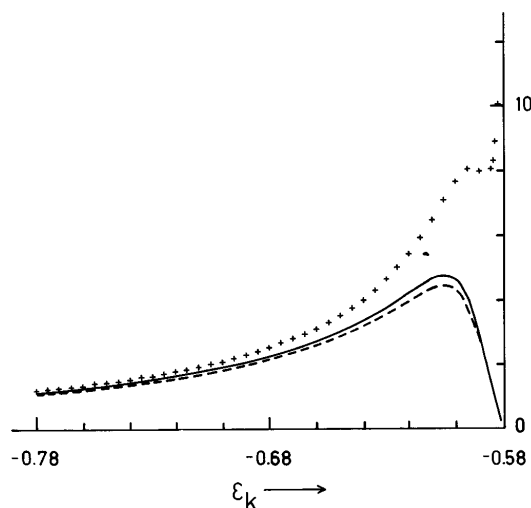


Figure 9. Bulk plasmon satellite spectra for $\omega = 8$, averaged over the position of the core level. The solid line shows the average as obtained with the theory here, the dashed line is from averaging with an exponential corresponding to the mean free path, and the crosses are from using the same exponential averaging but with a fluctuation potential as a plane wave combined with a step function at the surface. From reference [8].

$\propto \omega^{-(1-\alpha)}$, in a narrow region at threshold.

Results for different core distances from the surface are shown in figure 13. We see that we have to go to a distance of about 6 au before the bulk asymptotic limit is reached. The behaviour of α for very small z is unrealistic. We can however conclude that α is enhanced close to the surface.

5.4. Strongly correlated systems

In a recent work core-electron photoemission in a localized strongly correlated model system was studied [82]. In this case the sudden limit is reached on an energy scale of $1/(2\tilde{R}^2)$, where \tilde{R} is the length scale of the interaction potential. For the systems that we have in mind—transition metal and rare-earth compounds, chemisorption systems, and high- T_c compounds—this energy is only about 10 eV. The model system has three electron levels: one core level and two outer levels. In the initial state the core level and one outer level are filled (a spinless two-electron problem). When the core hole is created, the more localized outer level (d) is pulled below the less localized level (L). The spectrum has a leading peak corresponding to a charge transfer between L and d ('shake-down'), and a satellite corresponding to no charge transfer. The model has a Coulomb interaction between these levels and the photoelectron states.

We will discuss here extended quasi-boson-type excitations (related to the dielectric response function) when the localized system is embedded in a solid. The photoelectron can then create such excitations on its way out. Also the rearrangement of the localized system can give rise to such excitations. We are interested in energies above say 10 eV, when the localized system has reached its sudden limit. To specify the photocurrent amplitude we need an additional index i for the final state of the localized system, and equation (60) is replaced

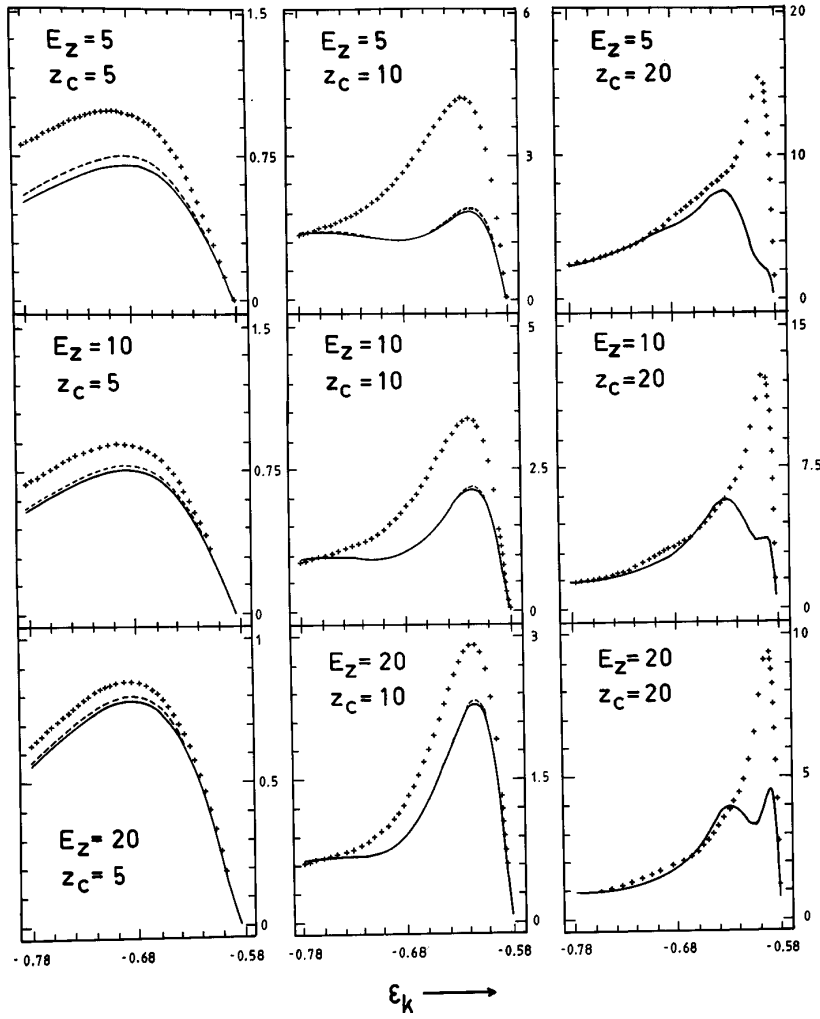


Figure 10. The bulk plasmon satellite for different photon energies E_z , and different distances z_c of the core hole from the surface. Solid lines: full calculation; dashed lines: backward propagation neglected; crosses: interference terms neglected. From reference [8].

by

$$\tau_{is}(\mathbf{k}) = \langle \tilde{\mathbf{k}} | T_{is} \Delta | c \rangle \quad T_{is} = \langle i, s | 1 + V \frac{1}{E - H + i\eta} | \Psi_0 \rangle. \quad (73)$$

The energy E is

$$E = \omega + E_0 = E_i + \sum_\nu \omega_\nu n_\nu(s) + \varepsilon_{\mathbf{k}}$$

where E_i is one of the final-state energies for the localized system ($i = 1, 2$). The initial and final states are of product form:

$$|\Psi_0\rangle = |\psi_0\rangle |\psi_{QB,0}^0\rangle \quad |i, s\rangle = |\psi_i\rangle |\psi_{QB,s}^i\rangle.$$

Here $|\psi_0\rangle$ is the ground state of the localized system, and $|\psi_{QB,0}^0\rangle$ the no-core-hole ground state of the quasi-boson system, while $|\psi_i\rangle$ is the i th final state (with a core hole) of the localized

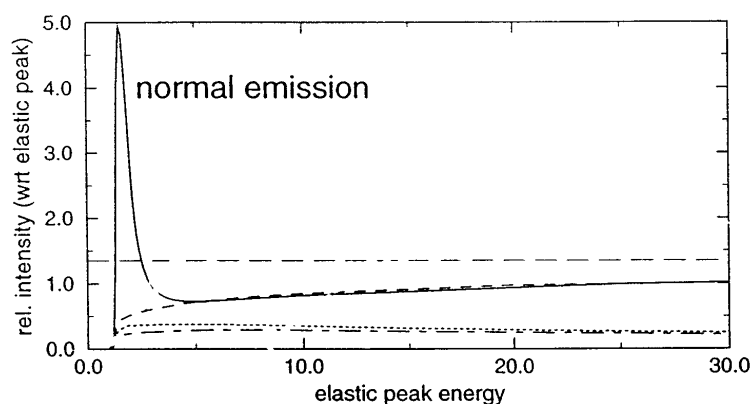


Figure 11. The total intensity of the bulk (upper two curves) and surface (lower two curves) plasmon satellites relative to the elastic peak intensity, as a function of the photon energy (= the energy of the elastic peak). From reference [14].

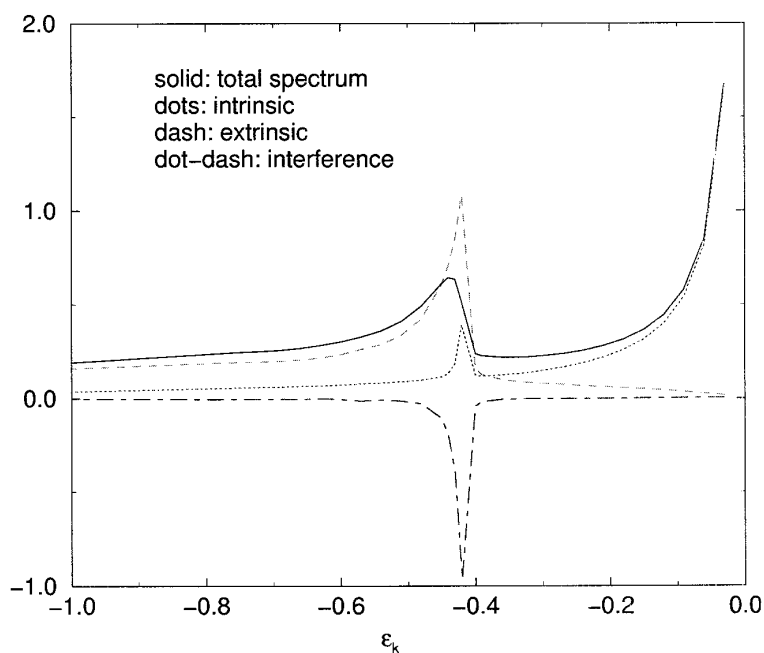


Figure 12. RPA results for particle-hole pairs plus surface plasmons for a photon energy of 5, and a core-hole distance from the surface of 20. Solid line: total spectrum; dots: intrinsic spectrum; dashed line: extrinsic spectrum; dot-dashed line: interference. From reference [14].

system, and $|\psi_{QB,s}^i\rangle$ is the s th state of the quasi-boson system, when the localized system is in state i . The potential V is $V = V_1 + V_2$, where V_1 describes the coupling of the photoelectron to the localized system, and V_2 that to the extended system. The Hamiltonian H is

$$H = H_0 + T + V \quad H_0 = H^{loc} + H^{QB}$$

where H^{loc} describes the localized two-level system discussed in [82], and H^{QB} is the Hamil-

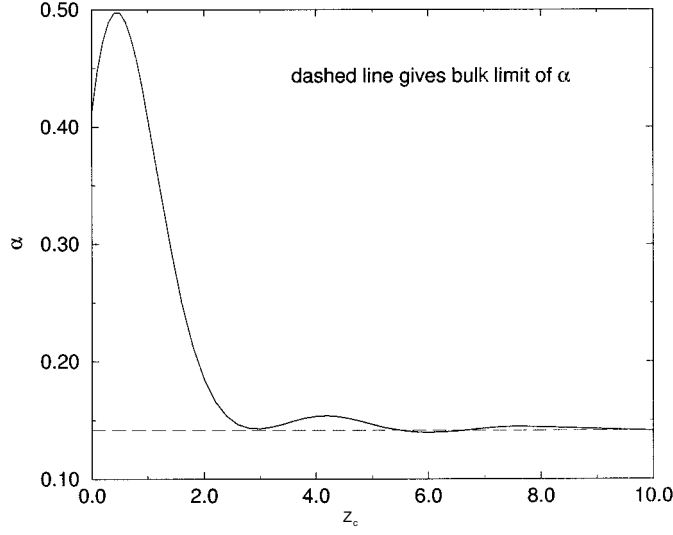


Figure 13. The singularity index α as a function of the core-hole distance from the surface z_c . The dashed line gives the bulk limit of α . From reference [14].

tonian for the quasi-boson system:

$$H^{loc} = \epsilon_a n_a + \epsilon_b n_b + \epsilon_c n_c + U_a n_c n_a + U_b n_c n_b + t(c_a^\dagger c_b + c_b^\dagger c_a)$$

where

$$H^{QB} = \sum_{\nu} \omega_{\nu} a_{\nu}^{\dagger} a_{\nu} + \sum_{\nu} (n_a V_{aa}^{\nu} + n_b V_{bb}^{\nu} + n_c V_{cc}^{\nu})(a_{\nu} + a_{\nu}^{\dagger})$$

$$V_1 = \sum_{kk'} (n_a V_{kk'}^a + n_b V_{kk'}^b - V_{kk'}^c) c_k^{\dagger} c_{k'}$$

$$V_2 = \sum_{\nu kk'} V_{kk'}^{\nu} (a_{\nu} + a_{\nu}^{\dagger}) c_k^{\dagger} c_{k'}$$

Here V_{aa}^{ν} etc are the aa etc matrix elements of the fluctuation potential $V^{\nu}(\mathbf{r})$ associated with the quasi-boson ν [14], while $V^a(\mathbf{r})$ etc are the (weakly screened) Coulomb potentials from the charge of orbital a etc [82]. In H^{QB} , n_a and n_b are true operators, unlike n_c which can be treated as a scalar. This makes our problem more difficult than the case treated in reference [14], where only n_c appears. To avoid this difficulty, we neglect the quantum fluctuations by taking appropriate expectation values of n_a and n_b . This means that we have three different H_i^{QB} corresponding to the ground state and the two excited states of the localized system. We define

$$H_i^{QB} = \langle \psi_i | H^{QB} | \psi_i \rangle = \sum_{\nu} \omega_{\nu} a_{\nu}^{\dagger} a_{\nu} + \sum_{\nu} V_i^{\nu} (a_{\nu} + a_{\nu}^{\dagger}) \quad (74)$$

where

$$V_0^{\nu} = \langle \psi_0 | n_a V_{aa}^{\nu} + n_b V_{bb}^{\nu} + V_{cc}^{\nu} | \psi_0 \rangle \quad V_i^{\nu} = \langle \psi_i | n_a V_{aa}^{\nu} + n_b V_{bb}^{\nu} | \psi_i \rangle \quad i = 1, 2.$$

$|\psi_{QB,s}^i\rangle$ is eigenstate s of the Hamiltonian H_i^{QB} . If we diagonalize the three different H_i^{QB} , we have three different bosons, $a_{i\nu}$:

$$a_{i\nu} = a_{\nu} + \frac{V_i^{\nu}}{\omega_{\nu}} \quad H_i^{QB} = \sum_{\nu} \left[\omega_{\nu} a_{i\nu}^{\dagger} a_{i\nu} - \frac{(V_i^{\nu})^2}{\omega_{\nu}} \right] \quad |\psi_{QB,s}^i\rangle = e^{-S_i} |\psi_{QB,s}^0\rangle$$

where the $|\psi_{QB,s}^i\rangle$ are eigenfunctions of H_i^{QB} , and $S_0 = 0$. Without this approximation the final states $|i, s\rangle$ are no longer a product $|\psi_i\rangle|\psi_{QB,s}^i\rangle$.

We can use the well-known scattering theory identity

$$\left[1 + \frac{1}{E - H_0 - T - V_1 - V_2 - i\eta}(V_1 + V_2)\right] = t_1 t_2$$

where

$$t_1 = \left[1 + \frac{1}{E - H_0 - T - V_1 - V_2 - i\eta}V_1\right]$$

$$t_2 = \left[1 + \frac{1}{E - H_0 - T - V_2 - i\eta}V_2\right].$$

to obtain

$$T_{is} = \langle i, s | t_2^\dagger t_1^\dagger | \Psi_0 \rangle.$$

Putting $V_1 = 0$ in t_1^\dagger (since the localized system has reached its sudden limit) gives

$$T_{is} = \langle \psi_{QB,s}^i | 1 + V_2 \frac{1}{E - E_i - H_i^{QB} - T - V_2 + i\eta} | \psi_{QB,0}^0 \rangle \langle \psi_i | \psi_0 \rangle \quad (75)$$

and

$$\tau_{is}(\mathbf{k}) = \langle \tilde{\mathbf{k}} | \langle \psi_{QB,s}^i | \left[1 + V_2 \frac{1}{E - E_i - H_i^{QB} - T - V_2 + i\eta}\right] e^{S_i} | \psi_{QB,0}^i \rangle \Delta | c \rangle \langle \psi_i | \psi_0 \rangle. \quad (76)$$

The calculation of $\tau_{is}(\mathbf{k})$ is now very similar to the problem discussed in [14]. For charge-transfer systems however, we have much more complicated fluctuation potentials to evaluate, but this is not a question of principle but of computational work. We can expect the intrinsic (shake-up) contribution from states of L character to be much larger than that from those of d character, where the d-electron and core-hole potentials largely cancel. The interference between intrinsic and extrinsic contributions is however strong only when we have a strong contribution from excitations with small \mathbf{q} (e.g. plasmons). For the type of system that we have in mind, the sharp plasmons which can appear have a very small strength, and thus we expect small interference effects, but not small extrinsic effects.

Since the surface-modified function $\text{Im } W(\mathbf{Q}, z, z'; \omega)$ in equation (65) is difficult to calculate, we want to relate it to its bulk counterpart. One, perhaps oversimplified, possibility is to write

$$\text{Im } W^{bulk}(\mathbf{Q}, z, z'; \omega) = \frac{1}{2\pi} \int e^{iq(z-z')} \text{Im } W^{bulk}(\mathbf{Q}, q; \omega) dq$$

and then make the replacement (cf. equation (72))

$$e^{iq(z-z')} \rightarrow F_q(z)F_q(z')$$

where

$$F_q(z) = \sqrt{2}[\cos(qz + \phi_q) - \cos \phi_q e^{-Qz}]$$

to obtain our desired $\text{Im } W$ as

$$\text{Im } W(\mathbf{Q}, z, z'; \omega) = \frac{1}{2\pi} \int F_q(z)F_q(z') \text{Im } W^{bulk}(\mathbf{Q}, q; \omega) dq.$$

It should be possible to combine data from optical absorption, energy loss, etc, and from RPA calculations to approximate $\text{Im } W^{bulk}(\mathbf{q}; \omega)$. Our theory would then allow quantitative evaluations for strongly correlated systems also.

6. Concluding remarks

The effects of electron correlation on spectroscopies like photoemission, electron scattering, and x-ray absorption are today treated in a rather incomplete way. We have discussed photoemission as a typical case in need of improvements. We have only studied zero temperature and not included any phonon effects. It should however be clear from our presentation that the approach can be adapted to all electron spectroscopies, to non-zero temperatures, and to include phonons. Our approximations are in the same spirit as the GWA. So far only very simple models have been studied, but it is an *a priori* approach allowing the one-electron aspects to be fully included.

We discuss a polaronic model Hamiltonian in detail, showing how its parameters can be calculated and how it gives the GWA in second-order perturbation theory. We show how to go beyond the GWA by summing a subset of diagrams for this Hamiltonian (this can also be regarded as the lowest-order cumulant approximation) to obtain an exponential expression which predicts the correct general behaviour for the intrinsic approximation of the core-electron photoemission spectrum. A model with fermions and bosons, where the bosons are built from fermions, clearly leads to double counting. This is a well-known situation from the Bohm–Pines electron gas theory [46], which in some respects is similar to ours. They also had the picture of electrons interacting with bosons (plasmons), and argued that the plasmon degrees of freedom were few, and thus that the subsidiary conditions which balanced the double-counting effects could be neglected.

The full expression for photoemission is analysed in the high-energy limit, and we show that again the same polaronic Hamiltonian can be used also to describe the extrinsic losses. These general results are applied to core-electron photoemission, leading to very simple expressions where the intrinsic amplitudes (those accounted for in the one-electron Green's function) and the extrinsic amplitudes add. Strong interference effects occur when there is a strong coupling to $q = 0$ bosons. This is typical for metals where the plasmons are the dominating bosons, and the approach to the sudden limit is then very slow, being of the order of keV. For systems where localized excitations are important there are no long-wavelength bosons, and the cancellation effects are much weaker [82].

We would also like to comment on the difference between the correlation problems for sp and df solids, and on the possibilities of using polaron models also for the latter. Clearly the GWA describing long-range charge fluctuations, and a Hubbard model focusing on local on-site correlations, which drive strong spin correlations, are two extremes. The GWA has the advantage that it describes the charge fluctuations in detail, and we all know what strong effects even tiny charge movements have. In the Hubbard model the Hubbard U describes the important on-site Coulomb forces, but U itself is not known. U deviates by a factor of two or more from its free-atom value, a deviation caused by charge rearrangements or screening in the solid. This reduction of the atomic U is usually estimated by constrained-configuration LDA band calculations. An additional problem with the Hubbard model is that U is taken as a constant, while intuitively we expect the effective U to vary with the state that we are describing, particularly if different states involve different charge distributions. In sp solids, correlation effects are not immediately striking, while for the df solids, they are glaringly present. This does not mean that they are small for sp solids; it just means that simple models can work well.

In recent work, strongly correlated systems were successfully treated in the dynamic mean-field theory with the following expression for the self-energy [11–13]:

$$\Sigma_{Q\sigma}^{SF}(i\omega_\nu) = \frac{\bar{U}^2}{\beta} \sum_{\mu\bar{\sigma}} \chi_{Q\bar{\sigma}\sigma}(i\omega_\mu) \mathcal{G}_{Q\bar{\sigma}}(i\omega_\nu - i\omega_\mu) + \frac{\bar{U}^2}{\beta} \sum_{\mu\bar{\sigma}} \chi_{Q\bar{\sigma}\bar{\sigma}}(i\omega_\mu) \mathcal{G}_{Q\sigma}(i\omega_\nu - i\omega_\mu).$$

Here $G_{Q\sigma}(i\omega_n)$ is the local dynamical Weiss effective field, and *both the longitudinal and transverse magnetic susceptibilities enter*. Without going into details, which would lead us away from the main theme of this article, we note that the self-energy has a GW structure, and can hence be derived from a polaron Hamiltonian, but now for electrons coupled to spin rather than charge fluctuations. Such self-energies were discussed in the early paramagnon work, e.g. by Doniach and Engelsberg [84], and by Berk and Schrieffer [85]. Explicit formulations in terms of electron–magnon Hamiltonians are found in the works by Davis and Liu [86], and by Kleinman [87]. More recently, the Schrieffer spin-bag approach has been considered; this is the same structure [88, 89]. The simplicity of the electron–magnon Hamiltonians in the literature depends on severe approximations, e.g. using the Hubbard Hamiltonian, and a generalization to a general case including bandstructure and coupling to charge fluctuations is far from trivial. Still, a lot more of the basic physics may be found from the electron–magnon model (involving both spin susceptibility functions) by anyone daring enough to look for it.

Acknowledgments

Some ideas of importance for this work were presented at a workshop on *Photoemission Lineshapes: the Sudden Approximation and Beyond*, at the Institute of Theoretical Physics in Santa Barbara, CA, April 1997. Constructive discussions, particularly with Jim Allen, Olle Gunnarsson, Walter Kohn, David Langreth, and Jerry Mahan, are gratefully acknowledged. Most of the picture presented in this article has however developed over a long time, and it has been a great personal satisfaction to put a number of loose ends together, and to sharpen the arguments given in the original papers. I am grateful to a large number of people with whom I have discussed this approach over the years. I would also like to thank Ferdi Aryasetiawan and Olle Gunnarsson for reading and commenting on the manuscript.

References

- [1] Hedin L 1965 *Phys. Rev.* **139** A796
- [2] Hedin L 1965 *Ark. Fys.* **30** 231
- [3] Hybertsen M S and Louie S G 1987 *Comment. Condens. Matter Phys.* **13** 223
- [4] Aryasetiawan F and Gunnarsson O 1998 *Rep. Prog. Phys.* **61** 237
- [5] Aulbur W G, Jönsson L and Wilkins J W 1999 *Solid State Physics* ed H Ehrenreich and F Spaepen (New York: Academic)
- [6] Farid B 1999 *Electron Correlation in the Solid State* ed N H March (Singapore: World Scientific) ch 3
- [7] Hedin L 1980 *Phys. Scr.* **21** 477
- [8] Bardyszewski W and Hedin L 1985 *Phys. Scr.* **32** 439
- [9] Fujikawa T and Hedin L 1989 *Phys. Rev. B* **40** 11 507
- [10] Aryasetiawan F, Hedin L and Karlsson K 1996 *Phys. Rev. Lett.* **77** 2268
- [11] Fleck M, Oles A M and Hedin L 1997 *Phys. Rev. B* **56** 3159
- [12] Fleck M, Liechtenstein A I, Oles A M, Hedin L and Anisimov V I 1998 *Phys. Rev. Lett.* **80** 2393
- [13] Fleck M, Lichtenstein A I, Oles A M and Hedin L 1999 *Phys. Rev. B* **60** 5224
- [14] Hedin L, Michiels J and Inglesfield J 1998 *Phys. Rev. B* **58** 15 565
- [15] Gross E K U and Dreizler R M (ed) 1995 *NATO ASI Series B* vol 337 (New York: Plenum)
- [16] Hedin L 1995 *Int. J. Quantum Chem.* **56** 445
- [17] Fulde P 1995 *Electron Correlations in Molecules and Solids (Springer Series in Solid State Sciences vol 100)* (Berlin: Springer)
- [18] Savrasov S Y 1996 *Phys. Rev. B* **54** 16 470
- [19] Hedin L and Lundqvist S 1969 *Solid State Physics* vol 23, ed F Seitz, D Turnbull and H Ehrenreich (New York: Academic) p 1
- [20] Almladh C-O and Hedin L 1983 *Handbook on Synchrotron Radiation* vol 1b, ed E Koch (Amsterdam: North-Holland) pp 607–904
- [21] Hybertsen M S and Louie S G 1986 *Phys. Rev. Lett.* **55** 1418

- Hybertsen M S and Louie S G 1986 *Phys. Rev. B* **34** 5390
- [22] Godby R W, Schlüter M and Sham L J 1986 *Phys. Rev. Lett.* **56** 2415
Godby R W, Schlüter M and Sham L J 1988 *Phys. Rev. B* **37** 10 159
- [23] Rohlfing M, Kruger P, Pollmann J 1993 *Phys. Rev. B* **48** 17 791
- [24] Shirley E L, Zhu X and Louie S G 1992 *Phys. Rev. Lett.* **69** 2955
Shirley E L, Zhu X and Louie S G 1997 *Phys. Rev.* **56** 6648
- [25] Shirley E L and Louie S G 1993 *Phys. Rev. Lett.* **71** 133
- [26] Shirley E L, Terminello L J, Klepeis J E and Himpsel F J 1996 *Phys. Rev. B* **53** 10 296
- [27] Shirley E L 1998 *Phys. Rev. B* **58** 9579
- [28] Schonberger U and Aryasetiawan F 1995 *Phys. Rev. B* **52** 8788
- [29] Surh M P, Louie S G and Cohen M L 1991 *Phys. Rev. B* **43** 9126
- [30] Blase X, Rubio A, Louie S G and Cohen M L 1995 *Phys. Rev.* **51** 6868
- [31] Zhu X J and Louie S G 1991 *Phys. Rev. B* **43** 14 142
- [32] Rubio A *et al* 1993 *Phys. Rev. B* **48** 11 810
- [33] Palumbo M, Reining L, Godby R W, Bertoni C M and Börnsen N 1994 *Europhys. Lett.* **26** 607
- [34] Zakharov O *et al* 1994 *Phys. Rev.* **50** 10 780
- [35] Hedin L 1991 *Nucl. Instrum. Methods Phys. Res. A* **308** 169
- [36] Strictly speaking, we should have had $\langle k | \Sigma_{\text{pot}}(E_k) | k \rangle$. Our approximation applies if we use a zero-order Green's function $G_k(\omega) = 1/(\omega - \varepsilon_k - \Delta E_k)$ with a shift ΔE_k to make $E_k = \varepsilon_k + \Delta E_k$ for all k , and not only on the Fermi surface. Alternatively, we can argue that if the differences $\Delta E_k - \Delta E_i$ are small compared to ω_s for the s -values of importance, the approximation should work.
- [37] Almladh C-O and von Barth U 1976 *Phys. Rev. B* **13** 3307
- [38] Born M and Heisenberg W 1924 *Z. Phys.* **23** 388
- [39] Ritchie R H and Marusak A L 1970 *Surf. Sci.* **4** 234
- [40] News D M 1970 *Phys. Rev. B* **1** 3304
- [41] Bechstedt F, Enderlein R and Reichardt D 1983 *Phys. Status Solidi b* **117** 261
- [42] von Barth U and Hedin L 1974 *Nuovo Cimento B* **23** 1
- [43] Quinn J J 1962 *Phys. Rev.* **126** 1453
- [44] Gygi F and Baldereschi A 1989 *Phys. Rev. Lett.* **62** 2160
- [45] Massidda S, Continenza A, Posternak M and Baldereschi A 1997 *Phys. Rev. B* **55** 13 494
- [46] Bohm D and Pines D 1953 *Phys. Rev.* **92** 609
- [47] Hubbard J 1957 *Proc. R. Soc. A* **243** 336
- [48] Ehrenreich H and Cohen M 1959 *Phys. Rev.* **115** 786
- [49] Lindhard J 1954 *K. Danske Vidensk. Selsk. Mat.-Fys. Meddr.* **28** 1
- [50] Gell-Mann M and Brueckner K A 1957 *Phys. Rev.* **106** 364
- [51] Quinn J J and Ferrell R A 1958 *Phys. Rev.* **112** 812
- [52] DuBois D F 1959 *Ann. Phys., NY* **7** 174
- [53] Holm B and von Barth U 1998 *Phys. Rev.* **57** 2108
- [54] Schöne W-D and Eguiluz A G 1998 *Phys. Rev. Lett.* **81** 1662
- [55] von Barth U and Holm B 1996 *Phys. Rev.* **54** 8411
- [56] Shirley E L 1996 *Phys. Rev. B* **54** 7758
- [57] Mahan G D 1994 *Comment. Condens. Matter Phys.* **16** 333
- [58] Del Sole R, Reining L and Godby R W 1994 *Phys. Rev. B* **49** 8024
- [59] Hindgren M and Almladh C-O 1997 *Phys. Rev. B* **56** 12 832
- [60] Hedin L and Lundqvist B I 1971 *J. Phys. C: Solid State Phys.* **4** 2064
- [61] Rice T M 1965 *Ann. Phys., NY* **31** 100
- [62] Eguiluz A G and Quong A A 1995 *Dynamical Properties of Solids* vol 7, ed G K Horton and A A Maradudin (Amsterdam: North-Holland)
- [63] Langreth D C 1970 *Phys. Rev. B* **1** 471
- [64] Lundqvist B I 1967 *Phys. Kondens. Mater.* **6** 193
- [65] Overhauser A W 1971 *Phys. Rev. B* **3** 1888
- [66] Migdal A 1958 *Sov. Phys.-JETP* **7** 996
- [67] Fowler W B 1966 *Phys. Rev.* **151** 657
- [68] Hedin L, Lundqvist B I and Lundqvist S 1971 *Electronic Density of States (NBS Special Publication No 323)* ed L H Bennet (Washington: US Government Printing Office) p 233
- [69] Mahan G D 1981 *Many Particle Physics* (New York: Plenum)
- [70] McMullen T and Bergersen B 1974 *Can. J. Phys.* **52** 624
- [71] Gunnarsson O, Meden V and Schönhammer K 1994 *Phys. Rev. B* **50** 10 462

- [72] Doniach S 1970 *Phys. Rev. B* **2** 3898
- [73] Müller-Hartman E, Ramakrishnan T V and Toulouse G 1971 *Phys. Rev. B* **3** 1102
- [74] Berglund C N and Spicer W E 1964 *Phys. Rev.* **136** A1030
- [75] Chew G F and Low F E 1956 *Phys. Rev.* **101** 1579
- [76] Feshbach H 1967 *Ann. Phys., NY* **43** 410
- [77] The $i\omega t$ term in equation (46) gives an energy shift $\Delta\varepsilon = \sum_v V_v^2(z_c)/\omega_v$. This z_c -dependent core-level shift was omitted by the choice of energy scale for ω ; cf. equation (57).
- [78] Tung C J and Ritchie R H 1977 *Phys. Rev. B* **16** 4302
- [79] Chastenet D and Longe P 1980 *Phys. Rev. Lett.* **44** 91
- [80] Inglesfield J E 1983 *J. Phys. C: Solid State Phys.* **16** 403
- [81] Gadzuk J W 1977 *J. Electron Spectrosc.* **11** 355
- [82] Lee J D, Gunnarsson O and Hedin L 1999 *Phys. Rev. B* **60** 8034
- [83] Chang J J and Langreth D C 1977 *Phys. Rev. B* **8** 4683
- [84] Doniach S and Engelsberg S 1966 *Phys. Rev. Lett.* **17** 750
- [85] Berk N F and Schrieffer J R 1966 *Phys. Rev. Lett.* **17** 433
- [86] Davis L C and Liu S H 1967 *Phys. Rev.* **163** 503
- [87] Kleinman L 1978 *Phys. Rev. B* **17** 3666
- [88] Kampf A and Schrieffer J R 1990 *Phys. Rev. B* **41** 6399
- [89] Kampf A P 1994 *Phys. Rep.* **249** 219